Analytical and numerical analysis of tides and salinities in estuaries; part II: salinity distributions in prismatic and convergent tidal channels

Kees Kuijper & Leo C. Van Rijn

Ocean Dynamics
Theoretical, Computational and Observational Oceanography

ISSN 1616-7341
Volume 61
Number 11

Ocean Dynamics (2011) 61:1743-1765
DOI 10.1007/s10236-011-0454-z

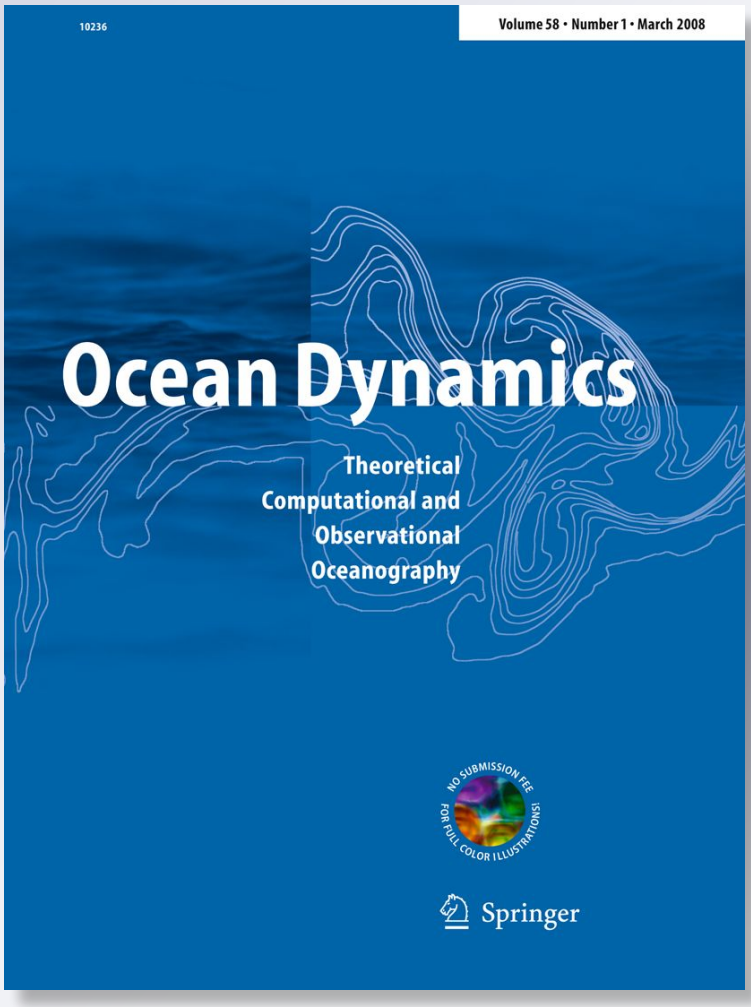

Springer

Your article is protected by copyright and all rights are held exclusively by Springer-Verlag. This e-offprint is for personal use only and shall not be self-archived in electronic repositories. If you wish to self-archive your work, please use the accepted author's version for posting to your own website or your institution's repository. You may further deposit the accepted author's version on a funder's repository at a funder's request, provided it is not made publicly available until 12 months after publication.

Springer

Author's personal copy

Ocean Dynamics (2011) 61:1743–1765
DOI 10.1007/s10236-011-0454-z

Analytical and numerical analysis of tides and salinities in estuaries; part II: salinity distributions in prismatic and convergent tidal channels

Kees Kuijper · Leo C. Van Rijn

Received: 3 February 2011 / Accepted: 9 June 2011 / Published online: 10 July 2011
© Springer-Verlag 2011

Abstract Estuaries, commonly, are densely populated areas serving the needs of the inhabitants in multiple ways. Often the interests are conflicting and decisions need to be made by the local managers. Intake of fresh water for consumption, agricultural purposes or use by industries may take place within a region not far landward of the limit of salt intrusion. Human interventions (e.g. deepening of the navigation channels) or climate changes (sea level rise, reduction of the river discharge) can bring these intake locations within the reach of saline or brackish water and consequently endanger their function. To support policy and managerial decisions, a profound knowledge of processes associated with the salinity structure in estuaries is required. Although nowadays advanced numerical three-dimensional models are available that are able to cope with the complexity of the physics there is still a need for relatively simple tools for quick-scan actions in a pre-phase of a project or for instructive purposes. The analytical model described in this paper may serve these needs. It computes the maximum salinity distribution using the dispersion coefficient in the mouth as the only model parameter. The model has been calibrated using observational data in a large number of estuaries and experimental data in a tidal flume. The dispersion coefficient was successfully related to geometric and hydrodynamic parameters resulting in an expression that can be used for convergent estuaries as well as prismatic channels, see Eqs. 25a and 25b. Application of the model in a predictive mode showed its promising capabilities. Comparison with three-dimensional numerical models indicates that the channel geometry in the estuary mouth largely influences dispersive processes. The analytical model for salt intrusion may be used in combination with the analytical model for tidal propagation in convergent estuaries and tidal channels by Van Rijn (part I). In this way, input is obtained on the tidal velocity amplitude and the Chézy roughness following calibration of this model on tidal amplitudes along the estuary.

Keywords Salinity · Convergent estuary · Prismatic channel · Analytical model · Numerical model · Tidal propagation

Responsible Editor: Roger Proctor

C. Kuijper (✉) · L. C. Van Rijn
Deltares,
Delft, The Netherlands
e-mail: kees.kuijper@deltares.nl

L. C. Van Rijn
e-mail: leo.vanrijn@deltares.nl

L. C. Van Rijn
University of Utrecht,
Utrecht, The Netherlands

1 Introduction

Salt intrusion in tidal estuaries often causes management problems as both the surface water and the groundwater are (partly) saline or brackish over substantial lengths along the estuary obstructing its use for drinking water and agricultural purposes (irrigation). These problems are enhanced when channel depths are increased by dredging to accommodate large vessels to nearby ports. To be able to quantify these effects on salt intrusion, it is necessary to know the basic relationships between salt intrusion and the hydraulic and geometric parameters involved.

The most important parameters influencing the maximum salt intrusion length at the end of the flood flow period in a tidal channel are the tidal characteristics (water level

Author's personal copy

amplitude and peak tidal velocity at the mouth), the river parameters (discharge and cross-section-averaged velocity) and the geometrical parameters (depth, width at mouth and width convergence length scale). At mid-latitudes, tidal parameters can vary over the 15-day spring–neap cycle. In these regions, the M2 tidal component generally predominates over the other constituents and, thus, variations on a time scale of 15 days are relatively small. The river discharge varies on the seasonal time scale (months) at most locations. The geometrical parameters generally do not vary much in time. Given these relatively large time scales involved, the salt intrusion process generally is in quasi-equilibrium on the tide-averaged time scale of 12 h. Hence, it is often allowed to use a tide-averaged approach to determine the salt intrusion length, as has been done by many authors (Ippen and Harleman 1961; Ippen 1966; Prandle 1981, 1985, 2004, 2009; Savenije 1986, 1989, 2005). Verification with observations should indicate whether such an approach is justified (Fischer et al. 1979). Ippen and Harleman (1961) introduced an elegant solution of the time-dependent salt continuity equation in a prismatic channel with partially mixed flow which is further discussed in Section 3.

Herein, the attention is focused on the maximum salt intrusion length occurring at high water slack (HWS) which is most relevant for management purposes. While tidal propagation in estuaries can be reasonably well described by linearized one-dimensional equations (see Van Rijn, part I), the physical and mathematical representation of saline intrusion tends to be much more complex.

Adopting a tide-averaged approach, the one-dimensional salt continuity equation can be expressed as a balance between the seaward-directed advective salt transport and the landward-directed dispersive or mixing-type transport. On a tide-averaged time scale the advective transport is caused by the fresh water discharge-related velocity (from the river), whereas the longitudinal dispersive-type transport is caused by tide-driven and density-driven processes. Tide-driven mixing encompasses a variety of processes such as (1) tidal trapping resulting from temporary storage of water in dead-end water bodies (see e.g. MacVean and Stacey 2011), (2) tidal pumping forced by residual circulation due to an irregular topography and the existence of ebb and flood channels (Fischer et al. 1979; Nguyen et al. 2008) and (3) tidal straining with convective overturning which is caused by the interaction of the vertical shear in the tidal current with the salinity field (Simpson et al. 1990; Prandle 2004). The dispersive transport reduces with the salinity gradient until it becomes zero near the toe of the salt front. Beyond the toe, the dispersion is dominated by small-scale turbulent mixing. Information on the relative importance of the various tide-averaged dispersion processes can be obtained by decomposing the velocity and salt concentration profiles taking residual flows over the depth and width into account. Using this approach, Fischer (1972) and Fischer et al. (1979) show that four dispersive terms can be distinguished: dispersive transport due to residual flow over the depth and over the width and shear flow effects (velocity gradient effects) over the depth and over the width. Scale analysis shows that the residual flows over the width yield by far the largest contribution. A major problem in the one-dimensional approach is that all dispersive processes must be represented by a single longitudinal dispersion coefficient D, which is hardly feasible (Prandle 1981). Recent developments in estuarine dispersive-type fluxes have been reviewed by Jay et al. (1997), concluding that there is a great lack of knowledge of dispersive processes in real estuaries and stressing that there is a need for additional research using controlled field experiments in combination with mathematical models.

So far, most studies have addressed the salt intrusion problem in prismatic channels. Salt intrusion in a tideless prismatic channel leads to an arrested salt wedge. This phenomenon has been studied extensively (Schijf and Schönfeld 1953; Keulegan 1966 and others). Salt intrusion in partially or well-mixed prismatic channels with tidal action has been studied experimentally and theoretically. Experimental research in long laboratory flumes has been done at Waterways Experimental Station in Vicksburg, USA (Ippen 1966) and at Delft Hydraulics in Delft, The Netherlands (Rigter 1973; Van Os 1993). Field data sets of salt intrusion have been collected at many sites, see summaries of Prandle (1985, 2004, 2009) and Savenije (1992, 1993a, 2005). Based on the laboratory data of Delft Hydraulics and field data of the Rotterdam Waterway, The Netherlands and the Chao Phya, Thailand, a relatively simple expression for the minimum salt intrusion length for prismatic channels has been proposed (Van Os 1993). This expression has been verified by Prandle (1985) by determining the tide-averaged length scale of a salt wedge based on the momentum equation. This latter approach represents the mean salt intrusion length rather than the minimum length. According to Prandle (2004, 2009) these expressions for the salt intrusion length in prismatic channels can also be used for convergent channels when the parameters involved (water depth, peak tidal velocity and fresh water velocity) are applied in the centre of the salt intrusion length. This requires, however, iterative computations, as the salt intrusion length is not known a priori.

Analytical salinity distributions for a prismatic tidal channel have been given by various authors (Ippen and Harleman 1961; Ippen 1966; Chatwin 1976; Prandle 1985, 2004, 2009; Savenije 1992, 2005). These analytical expressions always involve calibration coefficients related to the dispersive processes (dispersion coefficient in the mouth D_0 and other coefficients; Van der Burgh coefficient

Author's personal copy

K). Savenije proposed predictive expressions for the dispersion coefficient in the mouth (D_0) and the Van der Burgh coefficient K (the latter supposed to vary between 0 and 1). The effective longitudinal dispersion coefficient in saline tidal channels is much larger than the longitudinal dispersion coefficient in rivers, which is of the order of 0.1 to 1 $\overline{\overline{u}}h$ (Taylor 1954; Elder 1959). The vertical turbulence-induced mixing is of the order of 0.01 $\overline{\overline{u}}h$.

Prandle (1981) was one of the first to derive analytical salinity distributions for convergent channels (with depth and width variation) in combination with an analytical solution for the tidal wave propagation (based on Prandle and Rahman 1980). Analysis of field data of six estuaries resulted in D_0 values in the range of 50 to 500 m^2/s, but Prandle was not able to derive a rational dimensionless form for D_0 in terms of bulk estuarine parameters. Savenije (1986, 1989, 2005) also addressed salinity distributions in convergent tidal channels using the same approach as for prismatic channels. Channel convergence is represented by using an exponential function. Based on analysis of field data of 13 estuaries, he was able to propose a predictive expression for D_0 and the K parameter as function of bulk estuarine parameters.

The primary objective of the present analysis is to improve on this by considering both prismatic and convergent channels and reducing the empirical coefficients involved. The parameters for tidal wave propagation are taken from the analytical model for convergent and prismatic channels (see Van Rijn, part I). Using this approach, a relatively simple set of equations is obtained which can be used to get a first understanding of basic estuarine salinity processes, as is often required in the preliminary phase of estuarine projects. Recognizing the limitations of simple models, their main role is to better prepare the use of more detailed 2D and 3D mathematical models reducing the number of detailed runs.

The outline of the paper is as follows. In Section 2, the time-dependent one-dimensional transport equation for salt is considered. Starting from this equation the steady-state advection–dispersion equation is derived and flushing and dispersive time scales are estimated for conditions with increasing and decreasing river discharge. Section 3 presents the analytical model for salt intrusion in convergent estuaries as originally developed by Savenije (1986, 1989, 2005). In Section 4, the model is made suitable for prismatic channels as well and the so-called Van der Burgh parameter in the original model is assessed. The newly developed model is extensively calibrated using field observations and experimental data from flume studies (Section 5) and subsequently verified with data not used during calibration (Section 6). Furthermore, in Section 7 the analytical model is compared with advanced three-dimensional models. In this section, attention is focused on a schematized convergent estuary and the natural Scheldt estuary in The Netherlands. Finally, Section 8 summarizes the results and contains the conclusions of this work.

2 Basic considerations

We will start the analysis with the non-steady behaviour of the longitudinal salt distribution in accordance with the approach followed by Ippen and Harleman (1961) and Ippen (1966). The time-dependent one-dimensional salinity $\overline{\overline{S}}$ (−)[1] is described by:

$$\partial\left(\mathrm{A}\overline{\overline{\mathrm{S}}}\right)/\partial t+\partial\left[A\left(\overline{\overline{u}}_{\mathrm{tide}}-\overline{\overline{u}}_r\right)\overline{\overline{S}}\right]/\partial x-\partial^2\left(\mathrm{AD}\overline{\overline{\mathrm{S}}}\right)/\partial x^2=0 \tag{1}$$

with A the cross-sectional area relative to mean water level (m^2), t the time (s), $\overline{\overline{u}}_{\mathrm{tide}}$ the tidal velocity (m/s) flood is positive; ebb is negative), $\overline{\overline{u}}_r$ the fresh water velocity based on river discharge (m/s; negative in seaward direction), x the longitudinal coordinate (m; positive in landward direction) and D the dispersion coefficient (m^2/s). The double overbar in Eq. 1 indicates averaging over the cross section.

Ippen and Harleman (1961) and Ippen (1966) presented a solution of the *time-dependent* salt continuity equation in a prismatic channel with partially mixed flow conditions by splitting this equation in a time-dependent part and a steady-state part. Their steady-state solution described the salinity distribution at low water slack (LWS). The salinity distribution at high water slack (HWS) was obtained from the time-dependent solution. Their approach involved two calibration parameters: the dispersion coefficient D_0 at the mouth and the distance x_b seaward of the mouth where the salinity is equal to the maximum salinity at sea (S_0). Using laboratory flume data, the x_b value was found to be about 100 to 150 times the water depth at the mouth. They also showed that the migration distance of the saline front over the flood tide is approximately equal to the tidal excursion length (horizontal shifting of the salinity distribution).

To illustrate the time variation of the salinity profiles, a similar method (Van Rijn 1990, 2011) as that of Ippen and Harleman was calibrated and applied to the data (10 September 1979) of the prismatic Rotterdam Waterway, The Netherlands. Measured values are (Kuijper 1984): water depth, h_0=15 m; flow width, B=430 m; tidal velocity amplitude, $\hat{\overline{\overline{u}}}_0=0.6$ m/s; tidal period, T=45,000 s, river discharge, $|Q_r|$=1,160 m^3/s and density difference, $\Delta\rho_o$= 25 kg/m^3. The mouth (x=0) is taken at the opening of the

[1] Salinities are defined by the Practical Salinity Scale.

Author's personal copy

jetties which is about 4 km seawards of the coastline. As can be seen in Fig. 1, the minimum salt intrusion length is about 10 to 15 km at LWS and about 20 to 25 km at HWS. The computed salinity distributions are in reasonable agreement with measured values in the landward part of the channel after calibration of the dispersion coefficient at the mouth D_0 (=1,500 m^2/s) and the Van der Burg coefficient (K=0.5, see later). Deviations are largest close to the mouth (x=5 km). The computed minimum salt intrusion length is about 17 km, and the maximum value is about 26 km, which are in reasonable agreement with the observed values. The computed tidal excursion is approximately 9 km. The salinity distributions at various times are quite similar and in reasonable agreement with observed data. The tide-averaged salinity is the average of these salinity profiles.

The method of Ippen and Harleman clearly shows that the salinity at HWS can be obtained from that at LWS by shifting the salinity distribution over a length equal to the tidal excursion length in landward direction. A major drawback of the method applied is that measured data have to be available to calibrate the two coefficients involved. In the present research, it will be shown that the salinity distribution can be described by a simple analytical expression with only one calibration coefficient (dispersion at the mouth). A range of field data has been analysed to derive a predictive equation for the dispersion coefficient at the mouth.

Very often, a cross-section-averaged and tide-averaged approach is used to determine the salinity distribution and hence the salt intrusion length in an estuary with river inflow. This is most valid for *well-mixed conditions* (salinity is constant in vertical direction). Landward salt water intrusion in well-mixed conditions is caused by advective type and dispersive type of processes. When the river discharge remains constant for some time (>>tidal period T, say 10 days), the salt penetration length will become constant on a tide-averaged time scale. The salt penetration length will decrease for increasing fresh water discharge and increase for decreasing discharge.

Averaging the salt transport terms over the cross section and over time yields the balance equation for advective seaward salt transport and dispersive landward salt transport in stationary conditions as follows (river discharge should be constant for some time, say 10 days):

$$\left|\overline{\overline{u}}_r\right|\left\langle\overline{\overline{S}}\right\rangle + D\left\langle\partial\overline{\overline{S}}/\partial x\right\rangle = 0 \quad \text{or} \tag{2a}$$

$$|Q_r|\left\langle\overline{\overline{S}}\right\rangle + AD\left\langle\partial\overline{\overline{S}}/\partial x\right\rangle = 0 \tag{2b}$$

with $\left|\overline{\overline{u}}_r\right|$ the cross-section-averaged velocity (m/s) based on river discharge (=$|Q_r|/A$), $\overline{\overline{S}}$ the cross-section-averaged salt concentration (−), D the dispersion coefficient (m^2/s), Q_r the river discharge (m^3/s; fresh water), A=B h the area of cross section (m^2), B the average width of cross section (m), h=h_0 the average water depth to mean water level (m; assumed to be constant), < > the time-averaged value (averaged over the tidal period T). The boundary condition is $\left\langle\overline{\overline{S}}\right\rangle = S_0$ at the mouth.

Figure 2 shows various types of time-averaged and cross-section-averaged salt concentration distributions in a tidal estuary. The lower, exponential distribution (dashed line) is a concave distribution (rounded inward) and mainly occurs in prismatic estuaries. The upper distribution (dashed-dotted line) is a convex type of distribution (rounded outward) and occurs in large estuaries with a small river at the landward side (Scheldt estuary, The Netherlands; Thames estuary, England).

In the following the attention is focused on the salinity distribution at HWS (most landward salinity profile), which is of major importance for management purposes. For this condition, the tidal discharge is nil and the advection–dispersion equation takes its following form (Savenije 1989):

$$|Q_r|\overline{\overline{S}}_x^{\mathrm{HWS}} = -A_x D_x^{\mathrm{HWS}} \frac{\mathrm{d}\overline{\overline{S}}_x^{\mathrm{HWS}}}{\mathrm{d}x} \tag{3}$$

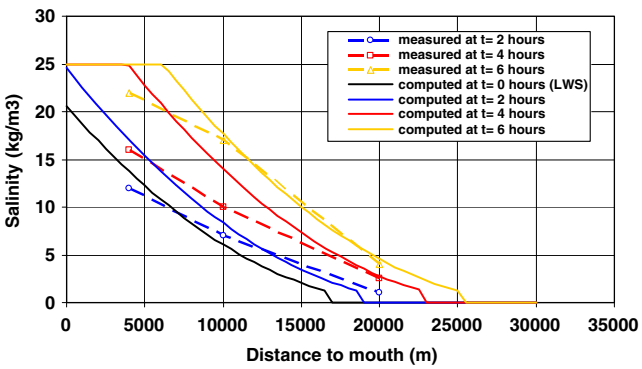

Fig. 1 Salinity distribution as function of time in prismatic channel, Nieuwe Waterweg, The Netherlands

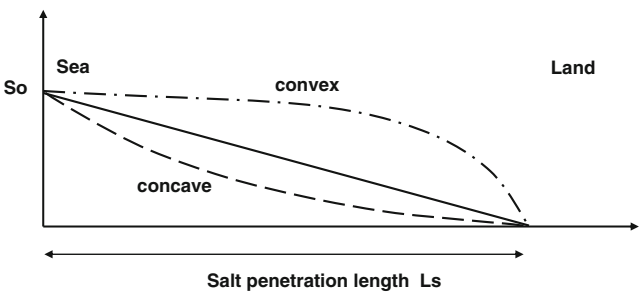

Fig. 2 Various types of tide-averaged salt concentration distributions in a tidal estuary

Author's personal copy

with Q_r the river discharge (m^3/s), S^{HWS} the salinity at high water slack (−), A the cross-sectional area (m^2), D^{HWS} the dispersion coefficient at high water slack (m^2/s). The longitudinal variation of the variables is denoted by the subscript x with x positive in landward direction. It is further assumed that the salinity of the river water can be neglected.

The salinity in an estuary channel can only be represented by the cross-section-averaged salinity if the lateral mixing proceeds relatively fast within the tidal cycle, which means that the channel width should be small compared with the tidal excursion length and width variations should be gradual. If these conditions are not satisfied, as is the case for some estuaries studied hereafter, then the applicability of a one-dimensional tide-averaged approach should be verified in practice.

Analysis of observed long-term salinity variations shows that the system reacts relatively quickly to a discharge increase and relatively slowly to a discharge decrease. The time scale of importance for the situation with a discharge increase is the flushing time to replace the salt water (over the salt intrusion length) by fresh water. Based on $dx = \overline{\overline{u}}_r dt$ and $h=h_0$=constant along the channel and $B = B_0 e^{-\beta x}$, with $\beta=1/L_b$=convergence coefficient (m^{-1}), the flushing time scale (T_{flush}) is:

$$\begin{aligned} T_{\text{flush, convergent}} &= \int_0^{L_s} \left(1/\overline{\overline{u}}_r\right) dx = (h_0/|Q_r|) \int_0^{L_s} B\, dx \\ &= (h_0 B_0/|Q_r|) \int_0^{L_s} e^{-\beta x}\, dx \\ &= (h_0 B_0/|Q_r|) L_b \left[1 - e^{-L_s/L_b}\right] \end{aligned} \tag{4a}$$

$$T_{\text{flush, prismatic}} = L_s \Big/ \left|\overline{\overline{u}}_r\right| \tag{4b}$$

These estimates for the flushing time are purely based on advection, which is in agreement with the ease that minimum, maximum and tide-averaged salt intrusion can be inter-related by simple tidal advection. The time scale of importance for the situation with a discharge decrease is the dispersive time scale, being the time required to move the salinity front over a length equal to the salt intrusion length L_s. Assuming an effective migration velocity of the salinity front in the tidal channel equal to $\langle u_{\text{eff}} \rangle \cong \left(D\, h\, \partial \overline{\overline{S}}/\partial x\right) \Big/ \left(h \overline{\overline{S}}\right) \cong D_0/L_s$, the time scale is:

$$T_{\text{dispersive}} = L_s/\langle u_{\text{eff}} \rangle = (L_s)^2/D_0 \tag{4c}$$

Using hydrodynamic characteristics for the Nieuwe Waterweg (see Table 1) the dispersion coefficient can be estimated as $D_0 \approx 3{,}000$ m^2/s resulting in a maximum salt intrusion length of 35 km (this paper). The time scale for adaptation of the salinity distribution in a prismatic channel due to an increase of the river discharge ($T_{\text{flush,prismatic}}$) amounts to approximately 2.5 days, whereas the dispersion time scale ($T_{\text{dispersive}}$) is in this case two times larger (≈5 days). Steady-state solutions can only be used when the time scale of the river discharge variations is much larger than those given by Eqs. 4a, 4b and 4c otherwise time-dependent solutions must be used.

3 Existing analytical model for salinity distribution in convergent estuaries

In this section first the salinity distribution in convergent estuaries will be described. The model was originally proposed by Savenije (1986, 1989, 2005) and makes use of two parameters: the longitudinal dispersion coefficient in the estuary mouth (D_0) and the so-called Van der Burgh parameter (K). According to Savenije (1993b, 2005), K varies between 0 and 1. Convergent estuaries are characterized by a cross-sectional area that decreases approximately exponentially going from the mouth of the estuary in landward direction. This change may be the result of an exponential decrease of either the width or the depth of the estuary or both. However in many cases the water depth can be considered approximately constant so that the converging lengths for the width and the cross-sectional area are equal. These types of estuaries are mostly alluvial, which means that the bed level has adapted to the governing hydrodynamic conditions. In contrast prismatic channels are mostly hydrodynamic systems that are human-made (e.g. access channels to inland harbours). The cross section is then uniform alongside the channel axis. A schematic figure illustrating symbols regarding salt intrusion is given in Fig. 3. Additional geometric and hydrodynamic parameters are given in Fig. 1 of part I on tidal propagation.

The cross-sectional area and the flow width of the estuary are described by exponential functions according to:

$$A_x = A_0 \exp(-x/L_a) \tag{5a}$$

$$B_x = B_0 \exp(-x/L_b) \tag{5b}$$

with A_0 the cross-sectional area (m^2) and B_0 the flow width (m) in the estuary mouth and L_a and L_b the convergence length scales (m).

Van der Burgh (1972) analysed a large number of measurements that were carried out between 1905 and 1971 on the Nieuwe Waterweg, which is a man-made prismatic channel (end of the nineteenth century) with an almost uniform cross section connecting the Port of

Author's personal copy

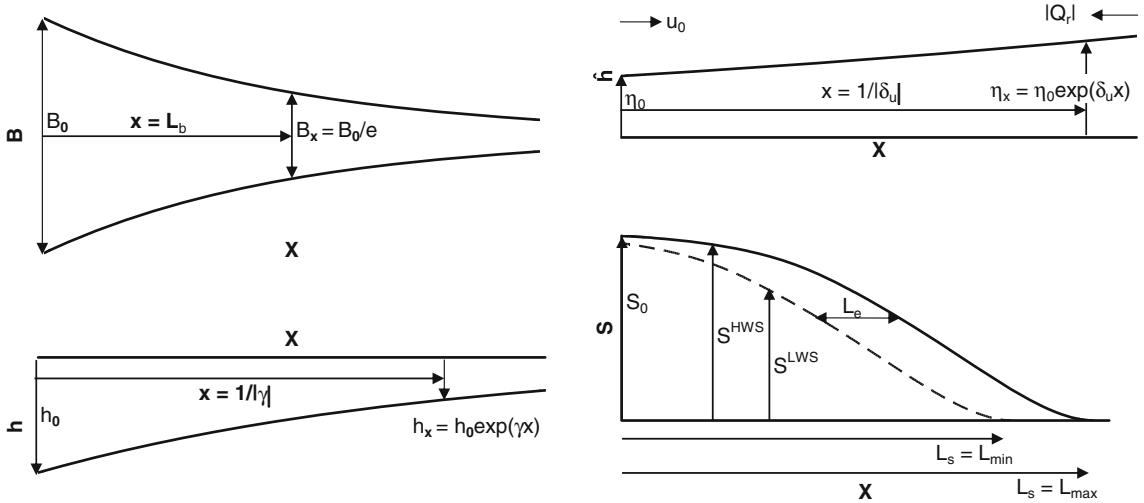

Fig. 3 Schematic sketch for characteristics on geometry, tide and salt intrusion in a convergent estuary. Longitudinal variation of width B (*upper left*), water depth h (*lower left*), tidal amplitude $\widehat{\eta}$ (*upper right*) and salinity S (*lower right*). Subscript '*0*' indicates estuary mouth; for additional symbols see text

Rotterdam with the North Sea. Van der Burgh proposed the following expression:

$$\frac{\mathrm{d}D_x}{\mathrm{d}x} = -K|u_r| = -K\frac{|Q_r|}{A} \tag{6}$$

with u_r the river discharge velocity (m/s) and A the cross-sectional area of the prismatic channel (m^2). If it is assumed that the Van der Burgh equation is also applicable to convergent channels it follows from Eqs. 3 and 6 that:

$$\frac{S_x}{S_0} = \left(\frac{D_x}{D_0}\right)^{\frac{1}{K}} \tag{7a}$$

with D_0 being the dispersion coefficient in the mouth (x=0). For reasons of simplicity, the superscript HWS has been omitted although the salinity S and the dispersion coefficient D as computed by the model will always relate to conditions at high water slack hereafter. Similarly the double overbar representing averaging over the cross section is left out of the equations.

Integration of Eq. 6 and using the expression for $A(x)$ according to Eq. 5a results in:

$$\frac{D_x}{D_0} = 1 - \frac{KL_a|Q_r|}{D_0A_0}\left[\mathrm{e}^{x/L_a} - 1\right] \tag{7b}$$

The maximum salt intrusion length $L_{\max}$ is obtained from Eq. 7b after substitution of D_x=0 at x=$L_{\max}$:

$$L_{\max} = L_a \ln\left(1 + \frac{D_0A_0}{KL_a|Q_r|}\right) \tag{8}$$

For the prismatic case ($L_a \to \infty$) Eq. 7b can be written as:

$$\frac{D_x}{D_0} = 1 - \frac{K|Q_r|}{D_0A_0}x \tag{9}$$

and the maximum salt intrusion length follows from:

$$L_{\max} = \frac{D_0A_0}{K|Q_r|} \tag{10}$$

where D_0 is assumed to have some finite value different from nil.

Savenije (1993a, 2005) applied the model to a large number of estuaries worldwide for which he was able to reproduce the salinity distributions very accurately using calibrated values for D_0 and K. Afterwards he derived relationships between each of these model parameters and geometric and hydrodynamic characteristics of the estuaries. For the dispersion coefficient in the estuary mouth, he found the following empirical relation:

$$D_0 = 1,400\, N_{R,0}^{0,5}\frac{L_{e,0}}{L_{a^*}}\widehat{u}_0\, h_0 \tag{11a}$$

with D_0 the dispersion coefficient at high water slack (m^2/s), $\widehat{u}_0$ the maximum tidal velocity (m/s), h_0 the water depth (m), $L_{e,0}$ the tidal excursion length (m) and $N_{R,0}$ the Estuarine Richardson number. All parameters are evaluated in the estuary mouth (x=0 m) as denoted by the subscript '0'. Because the water depth has been assumed constant, h_0 is equal to the mean water depth in the estuary. For some estuaries the cross-sectional area A_x was approximated by two different exponential functions with convergence lengths L_{a1} seaward and L_{a2} landward of x_1. Savenije used in these cases the weighted value for L_a (L_{a^*}) over the length of the salt intrusion L_s:

$$L_{a^*} = [L_{a1}x_1 + L_{a2}(L_s - x_1)]/L_s \tag{11b}$$

Author's personal copy

The Estuarine Richardson number in the estuary mouth ($N_{R,0}$) is defined by:

$$N_{R,0} = \frac{\Delta\rho g h_0}{\rho_r \widehat{u}_0^2} \frac{|Q_r|T}{P_{t,0}} = \frac{\pi \Delta\rho g h_0 |u_{r,0}|}{\rho_r \widehat{u}_0^3} \quad \text{using} \quad P_{t,0} = L_{e,0} A_0 = \frac{T\widehat{u}_0}{\pi} A_0 \tag{11c}$$

with g the gravitational acceleration (m/s^2), T the tidal period (s), $P_{t,0}$ the flood volume in the estuary mouth (m^3), $\Delta\rho$ the density difference between the sea and river water (kg/m^3) and ρ_r the density of the river water (kg/m^3).

It is noted here that D_0 according to Eq. 11a approaches nil if the convergence length L_a becomes infinitely large (the prismatic case) which is not realistic. Hence, this equation cannot be used for prismatic channels. The data used for the derivation of Eq. 11a limit the application of the equation to estuaries with $L_a/L_{e,0}$ between approximately 1 and 10 (i.e. $0.1<L_{e,0}/L_a<1$).

A predictive equation for the Van der Burgh coefficient K was more difficult to derive. Savenije (1993a, 2005) proposed an empirical relationship where K was related to many parameters amongst which the tidal excursion length, the tidal range, the roughness as given by Chézy, the convergence lengths for the width and the cross-sectional area and a parameter which accounts for tidal amplification or damping (δ_u).

4 Proposed modifications to the analytical model

The discussion of the analytical model in the previous section has raised the following questions:

1. Can we formulate a new analytical model based on D_0 only, thus eliminating the Van der Burgh parameter K?
2. Can we determine a general expression for D_0 which is valid for both prismatic and converging channels?

These topics will be addressed hereafter. Subsequently, the model is calibrated using experimental data in a tidal flume and observations in a large number of estuaries worldwide.

Firstly, we will adopt the following equations for the dispersion coefficient D_0 in the estuary mouth at high water slack for converging and prismatic channels.

$$D_0 = c_1\sqrt{\pi}\left(\frac{v_\Delta}{\widehat{u}_0}\right)^{\alpha_1}\left(\frac{C^2}{g}\right)^{\alpha_2}\left(\frac{|u_{r,0}|}{\widehat{u}_0}\right)^{\alpha_3}\frac{L_{e,0}}{L_a}\widehat{u}_0 h_0 \tag{12a}$$

(convergent)

$$D_0 = c_2\sqrt{\pi}\left(\frac{v_\Delta}{\widehat{u}_0}\right)^{\alpha_1}\left(\frac{C^2}{g}\right)^{\alpha_2}\left(\frac{|u_{r,0}|}{\widehat{u}_0}\right)^{\alpha_3}\widehat{u}_0 h_0 \tag{12b}$$

(prismatic)

$$v_\Delta = \sqrt{\frac{\Delta\rho}{\rho} g h_0} \tag{12c}$$

with C the Chézy roughness (m$^{0.5}$/s), α_1, α_2 and α_3 model parameters (−), c_1 and c_2 coefficients and the other quantities as defined before. It is noted here that Eq. 12a predicts a dispersion coefficient equal to zero if the converging length L_a approaches infinity (prismatic channel). As such the equation is only applicable for $1<L_a/L_{e,x}<10$, which is the range of values used by Savenije for the derivation of Eq. 11a for convergent estuaries. We assume that for prismatic channels ($L_a\to\infty$) the dispersion coefficient becomes independent of L_a and approaches a finite value given by Eq. 12b.

The ratio $|u_{r,0}|/\widehat{u}_0$ in Eqs. 12a and 12b has been identified by Prandle (1985) as an important parameter governing the level of stratification. The friction parameter C^2/g follows from energy considerations relating vertical mixing to the ratio of dissipated energy by means of bed friction and gained potential energy of the fresh river water due to an increase in density, see Ippen and Harleman (1961). Finally, the ratio $v_\Delta/\widehat{u}_0$ is introduced to describe the relative importance of the propagation velocity of a density current in relation to the maximum tidal flow velocity. Equation 12a is equivalent to the expression by Savenije according to Eq. 11a with c_1=1,400, α_1=1, α_2=0 and α_3=0.5. The values α_1=1 and α_3=0.5 are adopted hereafter and c_1, c_2 and α_2 will be determined in Section 5 by means of calibration using field data as well as experimental data from a straight flume.

Secondly, the dispersion coefficient according to Eqs. 12a and 12b are assumed to be valid locally. i.e. at each point within the range of salt intrusion. For convergent channels ($1<L_a/L_e<10$) D_x is expressed as:

$$D_x = c_1\sqrt{\pi}\left(\frac{v_{\Delta,x}}{\widehat{u}_x}\right)\left(\frac{C^2}{g}\right)^{\alpha_2}\left(\frac{|u_{r,x}|}{\widehat{u}_x}\right)^{0.5}\frac{L_{e,x}}{L_a}\widehat{u}_x h_x \quad \left(1<\frac{L_a}{L_{e,x}}<10\right) \quad \text{with } v_{\Delta,x} = \sqrt{\frac{\Delta\rho_x}{\rho} g h_x} \tag{13}$$

The river flow velocity $u_{r,x}$ is equal to Q_r/A_x. The amplitude of the tidal velocity $\widehat{u}_x$ in a convergent or prismatic channel (without reflection) has been derived by (Van Rijn, part I):

$$\widehat{u}_x = \widehat{u}_0 \exp(\delta_u x) \tag{14a}$$

Author's personal copy

with δ_u the coefficient for tidal damping or amplification (m^{-1}). Here δ_u is equivalent to $-\varepsilon$ with ε defined in Table 1 of part I. This coefficient can be easily determined from the longitudinal variation of the tidal amplitude $\widehat{\eta}_x$ (m):

$$\widehat{\eta}_x = \widehat{\eta}_0 \exp(\delta_u x) \tag{14b}$$

with $\widehat{\eta}_0$ the tidal amplitude in the mouth (m).

Furthermore, the density is assumed to be a function of salinity only and $\Delta\rho_x$ is approximated with:

$$\Delta\rho_x = c_x S_x \approx 0.78\, S_x \tag{15}$$

The cross-sectional area A_x and the flow width B_x are given by Eqs. 5a and 5b. Thus, the water depth h_x follows from:

$$h_x = h_0 \exp(\gamma x) \tag{16}$$

$$\gamma = \frac{1}{L_b} - \frac{1}{L_a}$$

with γ (m^{-1}) the inverse of the convergence length scale for the water depth.

Because the tidal excursion length $L_{e,x}$ is proportional to $\widehat{u}_x$ it also follows that:

$$L_{e,x} = L_{e,0} \exp(\delta_u x) \tag{17}$$

Substitution of Eqs. 14a and 15, 16, 17 in Eq. 13 and making use of the approximation $\sqrt{c_x/c_0} \simeq 1$ results in (for details see Appendix A):

$$D_x = e^{\Phi x} D_0 \sqrt{\frac{S_x}{S_0}} \tag{18a}$$

with

$$\Phi = \frac{\delta_u}{2} + \frac{3\gamma}{2} + \frac{1}{2L_a}. \tag{18b}$$

This equation shows that the dispersion coefficient may increase in landward direction if Φ is sufficiently large. If the water depth is approximately constant ($\gamma \cong 0$) this is achieved for strongly convergent estuaries with $\delta_u > 0$ and L_a relatively small.

Differentiating D_x with respect to x and combining the result with the transport equation for salt results in the following equation for the longitudinal salt distribution (see also Appendix A):

$$\frac{S_x}{S_0} = \left[1 - \frac{1}{2}\frac{|Q_r|\zeta L_a}{A_0 D_0}\left(e^{x/(\zeta L_a)} - 1\right)\right]^2 \qquad \left(1 < \frac{L_a}{L_{e,x}} < 10\right) \tag{19}$$

with $\zeta = 1/(1 - \Phi L_a)$

The maximum salt intrusion length follows from the condition that $S=0$ at $x=L_{\max}$:

$$L_{\max} = \zeta L_a \ln\left(1 + 2\frac{D_0 A_0}{\zeta L_a |Q_r|}\right) \tag{20}$$

Savenije (1992; 2005) found for converging estuaries the following expression, see Eqs. 7a and 7b:

$$\frac{S_x}{S_0} = \left[1 - K\frac{|Q_r|L_a}{A_0 D_0}\left(e^{x/L_a} - 1\right)\right]^{\frac{1}{K}} \qquad \left(1 < \frac{L_a}{L_{e,x}} < 10\right) \tag{21}$$

Equation 19 is very similar to Eq. 21 as derived by Savenije except that L_a is replaced by ζL_a and $K=0.5$. These modifications result from the fact that tidal amplification and tidal damping have been taken into account. It is noted that the number of model parameters is reduced from two (D_0 and K) to only one (D_0) because the Van der Burgh parameter K appears to take a constant value of 0.5.

A similar derivation can be done for the prismatic case resulting in the salinity distribution given by:

$$\frac{S_x}{S_0} = \left[1 - \frac{|Q_r|}{\delta_u A D_0}\left(e^{\frac{\delta_u x}{2}} - 1\right)\right]^2 \tag{22}$$

from which the maximum salt intrusion length $L_{\max}$ is computed according to:

$$L_{\max} = \frac{2}{\delta_u} \ln\left(\frac{\delta_u A D_0}{|Q_r|} + 1\right) \tag{23}$$

5 Model calibration

5.1 Prismatic channel

In the previous section it was found that the Van der Burgh parameter (K) is equal to 0.5. The proposed analytical model thus employs only one model parameter being the dispersion coefficient in the estuary mouth (D_0). D_0 is determined by means of calibration so that model results show optimal agreement with observed salinities. Equation 11a has been derived by Savenije (1993a, 2005) after calibration of his model with data from alluvial estuaries for which $L_{a,*}/L_{e,0}$ is less than 10. It is hypothesized that for much larger values the dispersion coefficient D_0 becomes independent of L_a and approaches a finite value. Unfortunately, this hypothesis cannot be tested properly as limited field data on salinity distributions in prismatic channels are available. Rigter (1973) published results of 35 experiments in a straight and horizontal tidal flume of Delft Hydraulics for which the convergence length scales L_b and L_a were infinitely

Author's personal copy

large. With these tests the hydrodynamic conditions such as tidal amplitude, bed roughness, tidal velocity, river discharge, water depth and salinity at sea were widely varied. Rigter (1973) presented only the minimum salt intrusion lengths but as we will focus on the intrusion lengths at high water slack maximum values were taken from the original report (Rigter 1971). Calibration of Eqs. 12b and 23 with the tidal flume data results in α_2= 0.5 and c_2=6. Computed versus observed maximum intrusion lengths are shown in Fig. 4, indicating that the model is well able to reproduce the experimental data. For further details on the calibration process reference is made to Appendix B.

5.2 Convergent estuaries

The dispersion coefficient D_0 in the mouth of a convergent estuary is obtained through calibration of the longitudinal salinity distribution according to Eq. 19 using observations on salinity along the estuary at high water slack. Figure 5 shows as an example the observed and computed longitudinal salinity distribution for the Scheldt in the Netherlands. The estuary is a typically funnel-shaped meso-tidal estuary with an average depth of 12 m in its seaward region, a width at its mouth of 14 km, a tidal range in the mouth of 4 m and a relatively low yearly averaged river discharge of 120 m^3/s. From the Estuarine Richardson number in the mouth ($N_{R,0}$) the Scheldt can be classified as well mixed in vertical direction. The ratio of the width and the tidal excursion length is in the order of 1 so that in lateral direction the salinity distribution may be non-uniform. For this particular case only monthly averaged salinities were available. As such salinities were computed at high water slack and shifted in seaward direction over half of the tidal excursion length.

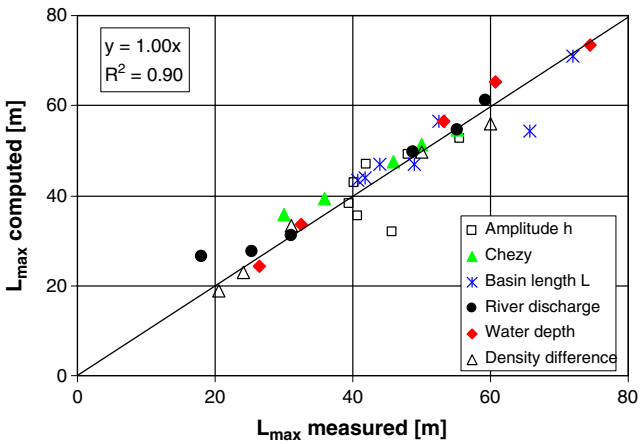

Fig. 4 Computed (Eqs. 12b and 23) versus measured maximum salt intrusion lengths in the tidal flume

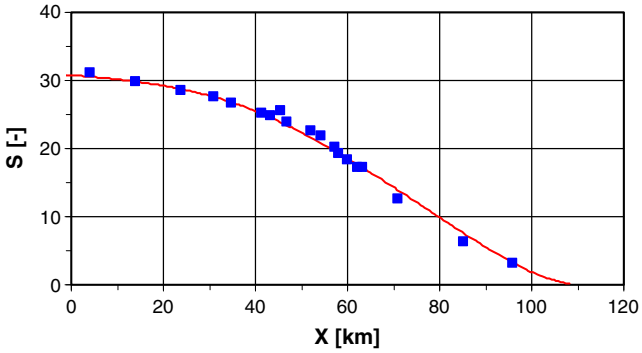

Fig. 5 Observed and computed salt distribution in the Scheldt estuary (October 1975, monthly averaged) after calibration with dispersion coefficient in the estuary mouth (D_0). *Symbols* observations. *Line* model

Results for 8 other estuaries are given in Appendix B although in total 23 different data sets are used during calibration. The Estuarine Richardson number in the mouth, $N_{R,0}$, indicates that according to Eq. 11c most of the estuaries can be classified as well mixed ($N_{R,0}$<0.08) or partially mixed (0.08<$N_{R,0}$<0.8). Only for four estuaries $N_{R,0}$ is slightly larger than 0.8, see Table 3. For a number of estuaries the estuary width is of the same magnitude as the tidal excursion length, or even larger, so that the salt distribution may be non-uniform in lateral direction. Computed versus observed salt intrusion lengths are shown in Fig. 6. The slope of the regression line is 1.03 with a regression coefficient of 0.96 indicating that the model is very well capable to hind cast salt intrusion lengths.

5.3 Synthesis

Results for the convergent case have been obtained with specific values of the dispersion coefficient in the estuary

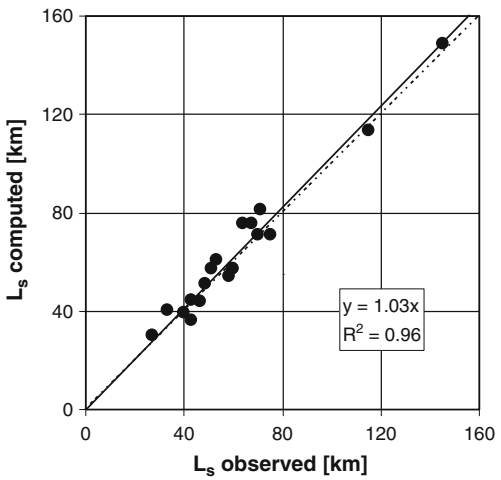

Fig. 6 Computed versus observed salt intrusion length (L_s) after calibration

Author's personal copy

mouth. To investigate the functional relationship according to Eq. 12a two dimensionless parameters are defined:

$$X = \frac{L_{a,*}}{L_{e,0}} \text{ and } Y = \frac{D_0}{\sqrt{\pi}\left(\frac{v_\Delta}{\widehat{u}_0}\right)^{\alpha_1}\left(\frac{C^2}{g}\right)^{\alpha_2}\left(\frac{|u_{r,0}|}{\widehat{u}_0}\right)^{\alpha_3}\widehat{u}_0 h_0}. \tag{24}$$

so that Eq. 12a takes the simple form of $Y=c_1\ X^{-1}$. Furthermore $\alpha_1=1$ and $\alpha_3=0.5$ following Savenije (1993a, 2005) while $\alpha_2=0.5$ as derived from the experimental flume data. Tidal velocities are computed with the analytical model proposed by Van Rijn (Van Rijn, part I). This is a first order approximation as the model is only applicable for situations with a constant water depth, which is not always true for the estuaries considered. Furthermore, if an estuary is schematised with two branches the tidal velocity amplitude in the mouth was computed with the geometric characteristics of the landward branch only. The Chézy roughness was determined by means of calibration of the analytical model on tidal propagation using data on the observed amplification or damping of the tidal range along the estuaries.

In Fig. 7, Y is given as a function of X on a log–log scale for all convergent estuaries used for calibration. Similar to Savenije (2005) the weighted value L_{a*} (see Eq. 11b) has been used for those estuaries that were schematized with two converging lengths L_{a1} and L_{a2}. For h_0 the average water depth along the estuary was selected rather than its value in the mouth. The reason is that the latter is not always known while an average value produced best results in deriving a predictive equation for D_0. Moreover, the tidal velocity amplitude ($\widehat{u}_0$) is computed with the analytical model by Van Rijn (part 1) which also assumes a constant water depth. Figure 7 also shows computed values for X and Y as derived from the tidal flume experiments in a prismatic channel. These data points should be positioned at infinite values of $L_a/L_{e,0}$ but for illustrative purposes they are given for the domain (100, 1,000).

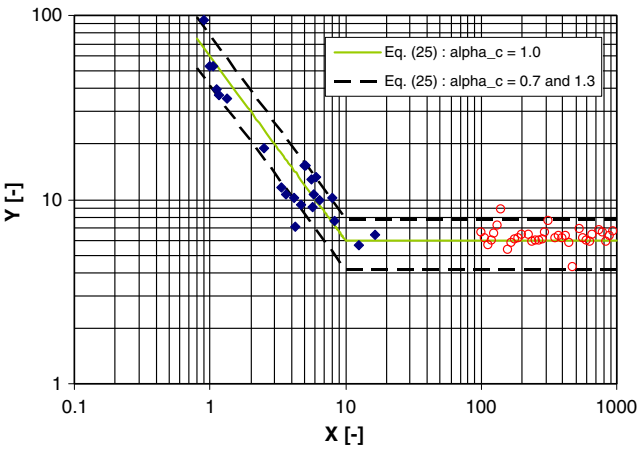

Fig. 7 Non-dimensional dispersion coefficient as a function of $L_a/L_{e,0}$ based on calibration for convergent estuaries (*triangles*) and prismatic channels (*circles*). X and Y are defined in Eq. 24. The predictive equation for D_0 (Eqs. 25a and 25b) is given by the *solid line* (α_c=1.0) and *dashed lines* (α_c=0.7 and 1.3)

For the convergent case the data points are adequately described by the proposed equation for D_0 according to Eq. 12a. Y increases from 6 to 60 if X decreases from 10 to 1 as indicated by the green line in Fig. 7 and consequently c_1=60. To account for the scatter calibration coefficient α_c is introduced with α_c varying between 0.7 and 1.3. Figure 7 further shows that the results of the flume experiments are consistent with the results obtained for alluvial convergent estuaries. The figure indicates that an estuary can be considered convergent if $L_{a,*}/L_{e,0}$ is less than approximately 10, whereas the prismatic case holds for larger values of $L_{a,*}/L_{e,0}$.

Thus for application of the model to convergent estuaries and prismatic channels the following equations for D_0 are proposed:

$$D_0 = \alpha_c 60\sqrt{\pi}\left(\frac{v_\Delta}{\widehat{u}_0}\right)\left(\frac{C}{\sqrt{g}}\right)\left(\frac{|u_{r,0}|}{\widehat{u}_0}\right)^{0.5}\widehat{u}_0 h_0\ \frac{L_{e,0}}{L_{a*}} \tag{25a}$$
$$\left(1 < \frac{L_{a*}}{L_{e,0}} < 10\right)$$

$$D_0 = \alpha_c 6\sqrt{\pi}\left(\frac{v_\Delta}{\widehat{u}_0}\right)\left(\frac{C}{\sqrt{g}}\right)\left(\frac{|u_{r,0}|}{\widehat{u}_0}\right)^{0.5}\widehat{u}_0 h_0 \tag{25b}$$
$$\left(\frac{L_{a*}}{L_{e,0}} \geq 10\right)$$

where v_Δ has been defined earlier with Eq. 12c and α_c (−) is an additional calibration factor with a default value equal to 1. Equations 25a and 25b with α_c is 0.7, 1.0 and 1.3 are shown in Fig. 7.

6 Model verification

The predictive capability of the model is assessed during verification. This particularly holds for Eqs. 25a and 25b as proposed in the previous section. The analytical model has been applied to a large number of convergent estuaries and prismatic channels using data that were not used during calibration. The data cover the same range as those used for calibration. Table 1 presents the relevant parameters for input and the dispersion coefficient in the estuary mouth (D_0) as predicted with Eqs. 25a and 25b. For these estuaries salinities over the intrusion length were available that allowed a detailed comparison with the results of the analytical model. The salinity distribution in the Thames was measured at low water slack. The model computation

Author's personal copy

Table 1 Estuaries used for verification of the model

Estuary	Date	L_{a1} and L_{a2} (km)	L_{b1} and L_{b2} (km)	x_1 (km)	T (s)	h_0 (m)	$\hat{\eta}_0$(m)	C^a ($m^{0.5}/s$)	$\hat{u}_0{}^a$ (m/s)	$\lvert Q_r\rvert$ (m^3/s)	S_0 (-)	A_0 (10^3 m^2)	N_R (-)	D_0^{pred} (m^2/s)	Reference
Thames	070449	19	26	–	44,440	7.1	2.15	75	1.10	40	31	51.3	0.003	508	Savenije (1992, 2005) and Hunt (1964)
Corantijn	020765	19, 64	19, 48	18	44,440	6.5	1.0	75	0.78	1,995	35	69	0.34	983	Savenije (1992, 2005)
Chao Phya	170380	109	109	–	86,400	7.2	0.75	60	0.47	43	35	4.3	0.58	353	Savenije (1992, 2005)
Chao Phya	280380	109	109	–	86,400	7.2	0.85	60	0.52	31	35	4.3	0.32	314	Savenije (1992, 2005)
Limpopo	100894	12, 72	12, 72	14	44,440	7.0	0.5	80	0.48	3	35	1.71	0.09	171	Savenije (1992, 2005)
Pungue	270202	20, 12	20, 14	38	44,440	3.5	3.05	55	1.29	200	29	28	0.008	418	Savenije (1992, 2005)
Maputo	020584	4, 16	4, 16	8	44,440	3.6	1.7	60	0.89	70	29	40	0.006	258	Savenije (1992, 2005)
Tha Chin	010386	22, 87	16, 87	22	86,400	5.3	0.9	45	0.46	40	35	3	0.61	353	Savenije (1992, 2005)
Incomati	100283	7, 42	7.5, 42	14	44,440	2.9	0.6	70	0.58	1	37	8.1	0.002	21	Savenije (1992, 2005)
Potomac	270478	53	69	–	44,400	9.2	0.2	75	0.19	270	11	160	0.57	193	Uncles (2002)
Potomac	230878	53	69	–	44,400	9.2	0.2	75	0.19	130	13	160	0.33	145	Uncles (2002)
Waterweg	100979	Prism.	Prism.	–	44,400	13.8	0.89	60	0.64	950	39	5.66	8.3	2,923	Kuijper (1984)
Yangtze	130204 220204	70	70	–	44,400	8	1.25	77	0.95	12,000	23	720	0.09	630	Chen (2001, 2002) and Xue (2009)
Minimum		4	4		44,440	2.9	0.2	45	0.19	1	11	1.71	0.002	21	
Maximum		109	109		86,400	13.8	3.05	80	1.29	12,000	37	720	8.3	2,923	

[a] Computed according to Van Rijn (part I)

Author's personal copy

was done for high water slack conditions and the resulting salinity distribution was shifted in seaward direction over the length of the tidal excursion. The salinity measurements in the Yangtze were performed in February 2004 (Xue et al. 2009). The river discharge during the measurements was not given so that it has been based on the long-term average discharge for this particular month as taken from (Chen et al. 2002). On the basis of the Estuarine Richardson number almost all estuaries can be classified as either well mixed or partially mixed. Only the Waterweg exhibits stratified conditions due to the large river flow velocity $|u_{r,0}|$ and large water depth h. The ratio between the width in the estuary mouth and the tidal excursion is in some cases in the order of 1 or even larger. For these circumstances the salinity distribution may be non-uniform in lateral direction.

The model is applied as follows:

1. Model input on geometric and bathymetric characteristics consists of the cross-sectional area A_0 in the mouth, the convergence length scales of the cross-sectional area L_a and the flow width L_b as defined by Eqs. 5a and 5b. The roughness in terms of the Chézy coefficient C is taken from the references as indicated in the last column of Table 1 or from calibration of the analytical model on tidal propagation by Van Rijn (part I).
2. Model input on hydrodynamic conditions are: the tidal velocity amplitude in the estuary mouth $\widehat{u}_0$, the tidal period T and the river discharge Q_r. If $\widehat{u}_0$ is unknown its value may be derived from a hydrodynamic model or, as in this paper, computed according to the analytical model for tidal propagation by Van Rijn (part I) using the tidal amplitude of the water level in the estuary mouth ($\widehat{\eta}_0$) and assuming a uniform water depth along the estuary. In the latter case the computation proceeds by iteration because first $\widehat{u}_0$ should be estimated due to the linearised friction term in the momentum equation for tidal propagation. In accordance with calibration the width convergence length of the landward branch has been used. From $\widehat{u}_0$, the tidal excursion length ($L_{e,0}$) is computed. The parameter for tidal damping or amplification (δ_u) as defined by Eqs. 14a and 14b follows from the analytical model by Van Rijn (part I) if the roughness C is known. It can also be estimated from the longitudinal variation of the observed tidal amplitude.
3. Model input on salinity concerns only the salinity in the estuary mouth (S_0). The salinity of the river water is assumed to be nil. With Eq. 15 the density difference between the sea and river water is computed. During verification the value for S_0 has been used as a degree of freedom in case that no measurements are available close to the mouth.
4. Finally, the dispersion coefficient in the estuary mouth (D_0) follows from Eq. 25a if $L_{a,*}/L_{e,0}<10$ or Eq. 25b otherwise and the longitudinal salinity distribution is computed with Eqs. 19 and 22, respectively.

The predictive equation for the dispersion coefficient in the mouth of a convergent estuary makes use of the weighted value of the convergence lengths (L_{a*}) if the variation of the cross-sectional area along the estuary is approximated with two exponential functions. A schematization of the estuary with only one exponential function for $A(x)$ may only be used if sufficiently accurate, otherwise this can result in large differences between observed and computed salinities. The schematization with two different exponential functions for $A(x)$ requires some iteration for step 4 (see above) as the salt intrusion length to compute L_{a*} is not known a priori. The computational procedure for step 4 is then as follows (see also Savenije 2005):

5. The total salt intrusion length is estimated and the equivalent convergence length L_{a*} is computed using the convergence lengths L_{a1} and L_{a2} for the seaward and landward branch which are connected at $x=x_1$, see Eq. 11b.
6. The dispersion coefficient in the mouth (D_0) then follows from Eqs. 25a and 25b with L_{a*} computed in the previous step. The salinity distribution for the seaward branch is computed with Eq. 19 using the convergence lengths L_{a1} and L_{b1} for this branch. The computed salinity at the node connecting both branches ($x=x_1$) is used as boundary condition for the landward branch. The salinity distribution for $x>x_1$ is computed with Eq. 19 using D_{x1}, A_{x1} and the convergence lengths L_{a2} and L_{b2} for this branch. The salt intrusion length for this branch (L_{s2}) relative to x_1 is computed with Eq. 20.
7. The maximum salt intrusion length $L_{\max}$ relative to the mouth is x_1+L_{s2}. It is compared with the initial estimate and a new computation is done until two successive values are within acceptable bounds. Usually, only a few iterations are needed.

Observed and predicted salinity distributions for some estuaries are given in Fig. 8 (solid lines). The tidal velocity amplitude in the estuary mouth has been computed with the analytical model for tidal propagation (Van Rijn, part I). Chézy values were determined by means of calibration of this model using observed data on tidal amplification and damping. Lower ($\alpha_c=0.7$) and upper bounds ($\alpha_c=1.3$) for the computed distributions are also shown in Fig. 8 (dashed lines).

Author's personal copy

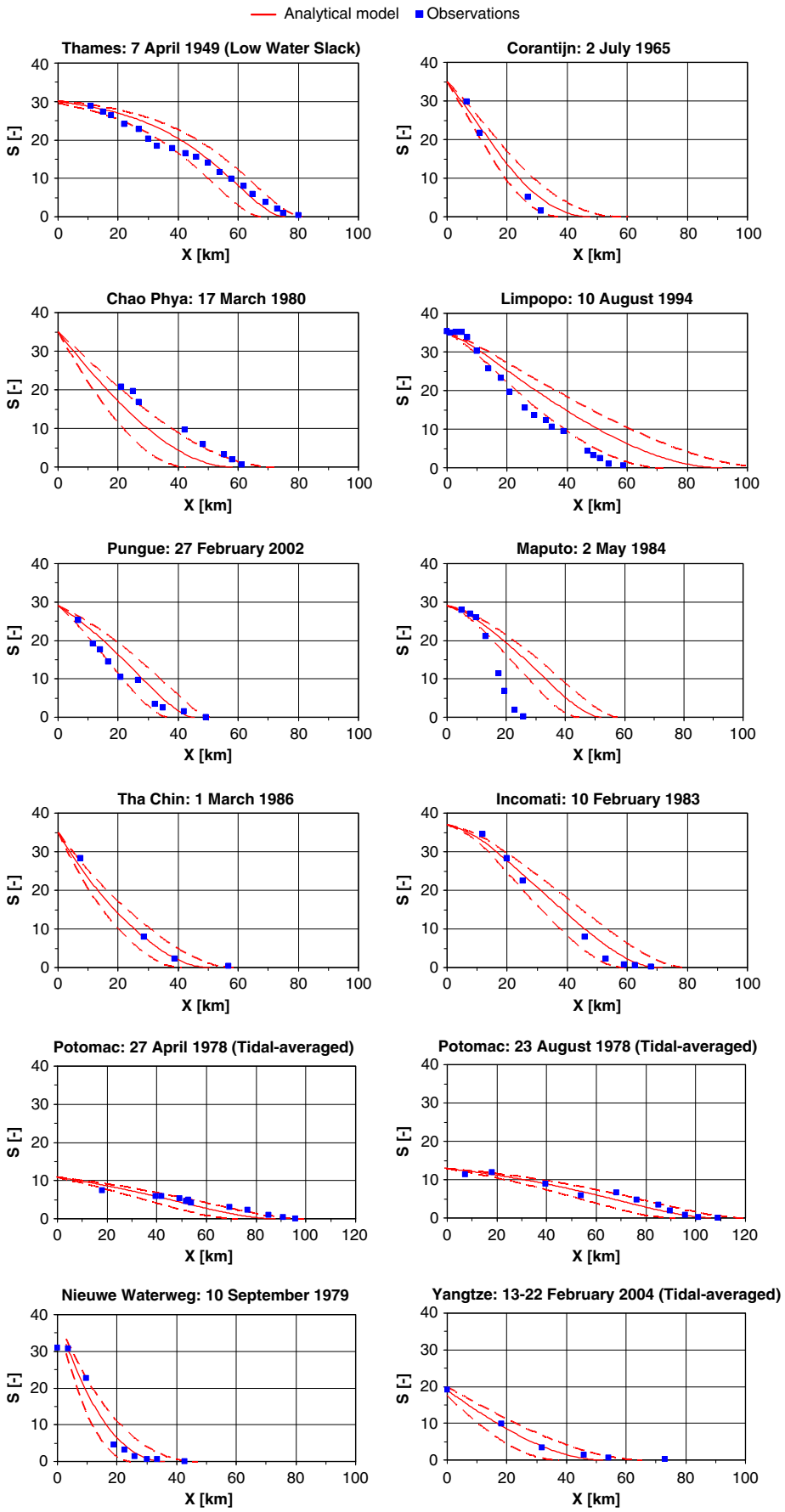

Fig. 8 Salinity distributions for estuaries based on verification (*solid lines*) including lower (α_c=0.7) and upper bounds (α_c=1.3) (*dashed lines*)

Author's personal copy

Figure 8 shows that the analytical model predicts in general quite well although for some estuaries differences may be large. It seems that the salinity structure in relatively short estuaries with strong convergence of the mouth resulting in limited intrusion lengths, such as the Maputo, cannot be captured satisfactorily by the model. In Fig. 9, the computed maximum salt intrusion lengths are compared with the observed intrusion lengths for two values of the calibration coefficient α_c, see Eqs. 25a and 25b, showing that the model predicts salt intrusion lengths reasonably well in the range of 30–150 km. The model performs somewhat better for α_c=0.95 as the model slightly overpredicts salt intrusion lengths. Only those data sets on salinity distribution have been used that allowed an accurate estimate of the maximum intrusion length, thus for measurements that have been performed near the toe of the salt wedge.

During calibration and verification, the salinity at the seaward boundary was taken equal or close to 35 for most of the estuaries. However, if the river discharge is large the salinity during high water slack in the estuary mouth may be less than ocean salinity and for predictive purposes the model should be supplied with additional information on how the salinity is related to the river flow. An option is to extend the model in seaward direction or to model explicitly the mixing processes in the coastal area near the mouth, see e.g. Ippen and Harleman (1961) and MacCready (2004). Such an extension of the model may be not feasible if the estuary forms part of a large water system. For instance, the salinity in the mouth of the Corantijn, which forms the border between Surinam and Guyana, is largely influenced by the river discharge of the Amazone 1,000 km to the east. Another example is the Potomac for which the salinities at its mouth are governed by the processes in Chesapeake Bay and thus have values that are much lower than ocean salinity.

7 Comparison with three-dimensional numerical models

The analytical model was further validated using results from two advanced numerical models: the Delft3D software of Deltares and the TRIWAQ programme of Rijkswaterstaat. In both cases, three-dimensional simulations were performed. First, the Delft3D model was used to simulate the salt intrusion in a prismatic channel with a length of 115 km, a width of 430 m and a mean water depth of 13.8 m. The tide at the sea boundary was varied according to a single harmonic function with a period of 12.5 h. The salinity at sea was maintained at a constant value of 28. At the landward end of the channel the tidal discharge was nil and a constant fresh river discharge was imposed. The tidal amplitude was varied between 0.5 and 1.2 m, the river discharge between 700 and 1,900 m^3/s and the water depth between 12 and 16 m. In total, seven model tests were compared. The resulting maximum salt intrusion lengths varied between 18 and 34 km while the minimum intrusion lengths were between 7 and 21 km. The minimum intrusion lengths were derived from the computed maximum values by subtracting the tidal excursion length. The average difference between the computed intrusion lengths by the analytical and numerical model was −0.9 km with a standard deviation of 1.2 km. Regression analysis resulted in r^2=0.98 indicating that the analytical model is very well capable to reproduce the 3D numerical results.

Next, the analytical model and Delft3D were compared for a schematic funnel-shaped estuary connected to a prismatic channel, see Fig. 10. The lengths of the convergent and prismatic sections were 60 and 120 km, respectively, and a uniform water depth of 10 m was assumed. The Nikuradse roughness was 0.05 m resulting in a Chézy value of 60 $m^{0.5}/s$. The estuary width in the mouth amounted 25 km. Convergence lengths for the cross-sectional area and the width were 25 km giving a channel width of 2,270 m between x=60 km and x=180 km. At the

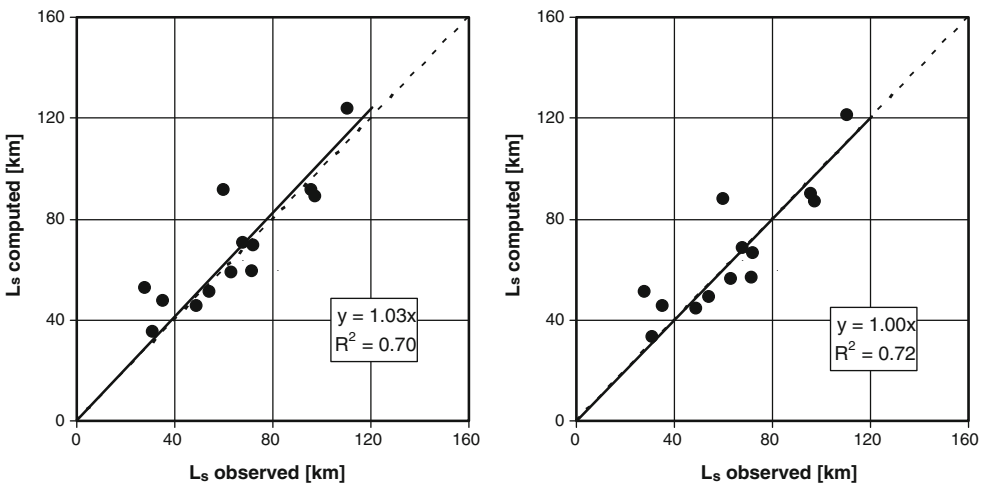

Fig. 9 Computed versus observed maximum salt intrusion length after verification with α_c=1.0 (*left panel*) and α_c=0.95 (*right panel*)

Author's personal copy

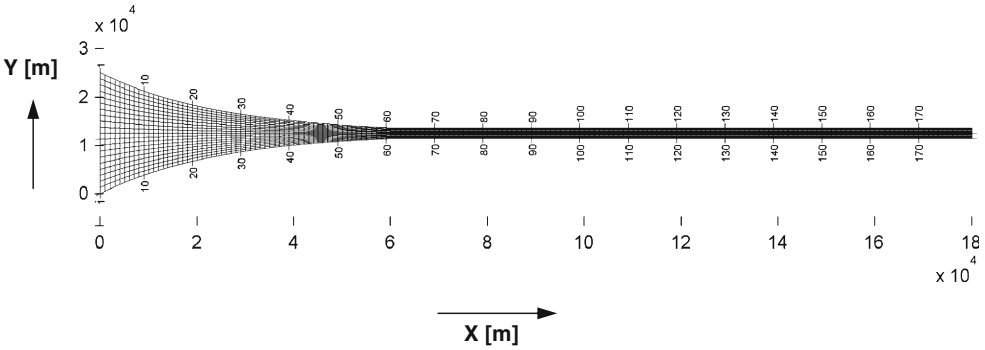

Fig. 10 Computational grid of Delft3D for schematized estuary

seaward boundary a harmonic varying water level with amplitude of 2.1 m was imposed. The landward end was closed with only a constant river discharge of 1,000 m^3/s. Salinities of sea and river water were 32 and nil, respectively. The numerical model employed ten equidistant computational layers and the number of grid cells in lateral direction was 20. The computational grid for the numerical model is also shown in Fig. 10. An additionally prescribed horizontal dispersion coefficient was varied in the range of 1 to 1,000 m^2/s being equal for longitudinal and lateral direction.

Computed isohalines were perpendicular to the longitudinal direction indicating a uniform salinity distribution in each of the cross sections. Also in vertical direction, the schematised estuary can be regarded as partially to well mixed ($N_{R,0}$=0.08). Using a turbulence-related dispersion coefficient of 1 m^2/s, the computed salinity distribution of the Delft3D model showed a large discrepancy with the distribution obtained with the analytical model. In the latter case the predicted intrusion length was much larger (>60 km) than the total length of the converging section whereas Delft3D computed that saline water did not even enter the prismatic channel (intrusion length, <60 km). Results of the numerical simulations based on additional horizontal dispersion coefficients (D_h) of 1, 100 and 1,000 m^2/s are shown in Fig. 11 (solid lines). The results with D_h=10 m^2/s (not shown) are almost similar to the run with D_h=1 m^2/s.

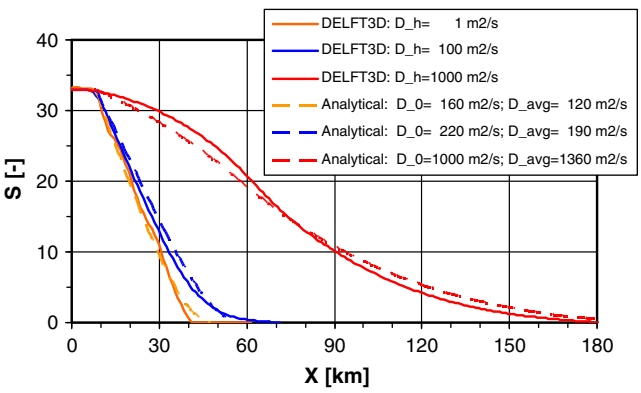

Fig. 11 Results of Delft3D based on horizontal dispersion of 1, 100 and 1,000 m^2/s (*solid lines*). Analytical results are obtained after calibration with D_0 (*dashed lines*)

The longitudinal salinity distribution from Delft3D was reproduced by the analytical model through calibration of the dispersion coefficient D_0 in the estuary mouth, see also Fig. 11 (dashed lines). Calibration of the analytical model for the run with almost no additional dispersion (D_h=1 m^2/s) resulted in an average dispersion over the salt intrusion length (D_{avg}) of 120 m^2/s. This can be considered as dispersion apparently present in the numerical model representing vertical circulation and other effects. The increased horizontal dispersion from 1 to 10 m^2/s in Delft3D is relatively small compared with what is already present and thus the salinity distribution is hardly affected by this. A further increase of the additional horizontal dispersion to 100 m^2/s does have effect on the salinity distribution because the total dispersion in the numerical model is approximately doubled. The average dispersion coefficient in the analytical model (D_{avg}) following from calibration then amounts 190 m^2/s. However an intrusion length of approximately 180 km as predicted by Eqs. 25a and 25b (D_0=1,000 m^2/s giving D_{avg}=1,360 m^2/s) can only be achieved if in Delft3D an additional horizontal dispersion of 1,000 m^2/s is included. The discrepancy between both models is attributed to the 'smoothness' of the schematized estuary (symmetric shape and constant depth). Contrary to natural alluvial estuaries, the schematisation lacks the presence of ebb, flood and connecting channels. It is believed that such a geometry promotes large-scale mixing thus enhancing dispersion (see e.g. Savenije 2005; Nguyen et al. 2008). The analytical model implicitly accounts for this because the predictive equation for D_0 is actually based on data from natural estuaries. We thus conclude that Eq. 25a is only applicable to natural systems with an irregular bathymetry consisting of multiple channels. The existence of such a system is believed to depend on the width-depth ratio (Allersma 1994; Savenije 2005; Toffolon and Crosato 2007).

To verify this hypothesis, the analytical model was also compared with numerical simulations for the Scheldt

Author's personal copy

estuary. Contrary to the simulations discussed above a realistic bathymetry was included in the model. Van Kessel and Vanlede (2010) carried out numerical simulations on mud dynamics in the Scheldt estuary using the three-dimensional TRIWAQ model of Rijkswaterstaat of the Ministry of Transport and Public Works of The Netherlands for the computation of the hydrodynamics. The model was run for a period of three months from 1 October 2006 to 1 January 2007 using six non-equidistant layers in the vertical direction. Actual boundary conditions were applied. Figure 12 shows the computed salinity distribution along a trajectory in the thalweg from Vlissingen (x=15 km) to beyond Rupelmonde (x=115 km). The salinity distribution is shown on 23 October at 08:00 h which is at the end of a period of 12 days with the river discharge in a absolute sense gradually decreasing to 37 m^3/s. Using the analytical model, the salinity distribution was computed with the converging lengths for the cross-sectional area and the width as used during calibration for the Scheldt (see Table 3). The river discharge was taken as 37 m^3/s (negative in seaward direction) and the calibration coefficient α_c in Eqs. 25a and 25b was successively set at 0.7, 1.0 and 1.3 resulting in dispersion coefficients in the estuary mouth of 230, 330 and 430 m^2/s.

Comparison of results from both models shows that the analytical model reproduces the results from the numerical model adequately. Apparently inclusion of the actual bathymetry in the numerical simulation leads to a representation of the horizontal dispersion which is in agreement with the prediction of the analytical model. It emphasizes the importance of the bathymetry on large-scale mixing processes, which was missing in the simulations for the schematized estuary as discussed before. The tidal forcing results in ebb-dominated and flood-dominated channels with a residual flow pattern after averaging over the tidal cycle. Mixing between these channels gives rise to an additional tide-driven dispersion known as tidal pumping

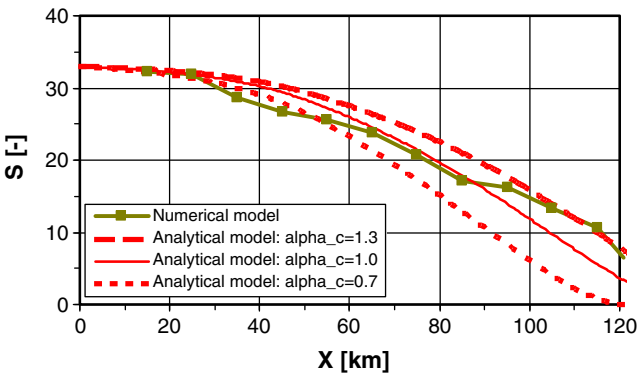

Fig. 12 Salinity distribution on 23 October at 08:00 h in the Scheldt estuary according to the numerical and the analytical model for three values of the calibration coefficient α_c

with a substantial contribution to salt intrusion in estuaries. These findings are in agreement with results of the analytical approach by Nguyen et al. (2008) who came to the conclusion that tide-driven dispersion is predominant over density-driven dispersion in relatively wide converging estuaries with a well-developed channel system.

8 Summary and conclusions

Methods have been developed previously to address issues on either the salinity structure in natural convergent estuaries or in prismatic tidal channels. The approach traditionally followed is that of tide averaging and cross-sectional averaging resulting in a steady one-dimensional equation for the salinity. The prescription of the dispersion appears to be the major factor controlling whether or not the model is able to describe the salinity distribution in estuaries. Given the multiple complicated processes regarding the interaction between the actual non-steady flow and salinity fields it may be expected that the inclusion of processes such as tidal pumping, tidal trapping and tidal straining in one single parameter is hardly feasible. Nevertheless, simple models like these haven been reasonably successful especially if the empiricism introduced is based on physical reasoning enhancing their predictive capability. The newly proposed analytical model is based on the original model by Savenije for convergent estuaries (1986, 1989, 2005) and computes the longitudinal salinity distribution at high water slack. The model takes tidal amplification and tidal damping resulting from convergence and friction explicitly into account. With the present research it has been shown that the two model parameters in Savenije's model (D_0 and K) can be reduced to only one being the dispersion coefficient in the estuary mouth (D_0) while the so-called Van der Burgh constant (K) takes a constant value of 0.5. Furthermore, the functional relationship between D_0 and the geometric and hydrodynamic parameters was extended to those of prismatic tidal channels enlarging the range of conditions for which the model can be applied. For this purpose, data from field surveys as well as measurements in a tidal flume were used.

Calibration of the model resulted in excellent reproduction of the maximum salinity distribution in a large number of convergent estuaries and prismatic channels for a wide range of conditions resulting in maximum salt intrusion lengths (L_{max}) between 30 and 150 km. As such, it is believed that the physics are captured to a large extent by the model parameterisation, although additional salinity measurements may be needed to reduce uncertainties in the model input. Calibrated values for the dispersion coefficient in the mouth were used to derive an equation that predicts D_0 as a function of geometric and hydrodynamic parameters, see Eqs. 25a and

Author's personal copy

25b. In some cases, two branches were needed to represent the actual geometry of the estuary. The empirical relationship for D_0 then requires a weighted convergence length scale of the cross-sectional area ($L_{a,*}$) to improve its predictive capability. This approach is however conflicting with the model assumption that the dispersion coefficient along the estuary is a function of local parameters only, see Eq. 13, and further research is needed to explain the inconsistency. Verification of the model using the predictive equation for D_0 showed in general good agreement between observed and computed salinities. Uncertainties in predicted values for D_0 appeared to be approximately ±30%. The salt intrusion in relatively short estuaries with strong convergence, like the Maputo, seems to be over predicted by the model.

The tide-averaged approach limits the applicability of the model to steady-state conditions which may not always apply especially for periods with decreasing river discharge when the time scale for adaptation of the salinity field is relatively large. Using the Estuarine Richardson number as indicator for the degree of stratification most of the estuaries considered during calibration and verification were classified as well mixed or partially mixed. Consequently, application of the model is justified for non-stratified conditions. Furthermore, it is expected that the one-dimensional approach is mostly valid if lateral salinity variations are small which is likely to occur if the estuary width is relatively small compared with the tidal excursion length. Although this condition was not always satisfied during calibration and verification the model results do not seem to be adversely affected hereby. Apparently, effects are accounted for by the computation of the dispersion coefficient. In some cases, model results were sensitive to the geometrical schematisation using exponential relationships for the cross-sectional area and the width (and, thus, for the water depth). Especially if data on geometry are scarce and scatter is substantial this may result in large uncertainties with respect to the model results. Notwithstanding its limitations the model can be helpful during the pre-phase of a project for screening purposes. The combination with the analytical model for tidal propagation in convergent estuaries (Van Rijn, part I) allows the assessment of tidal amplification or damping and the tidal velocity amplitude in the estuary mouth making the model predictive. Comparison with numerical model simulations showed the relevance of channel geometry for salt dispersion in relatively wide estuaries. The proposed equation for the dispersion coefficient in the estuary mouth implicitly accounts for this and application to systems lacking such a channel system may result in an over prediction of the salinity intrusion by the model.

Predictions for salinities during maximum intrusion can be easily converted to salinities during average or minimum intrusion by shifting the salinity distribution over half or the total tidal excursion length. Experiments in a (prismatic) tidal flume indicate that the maximum salt intrusion length as derived from an empirical expression for the minimum length and accounting for the tidal excursion length may even be a better procedure (see Appendix B). So far the application of this alternative approach to convergent estuaries has not been successful and further research is needed. Future research is also required to predict the salinity at high water slack in the mouth (S_0) during conditions with high river discharge. Field surveys to obtain data of salinity distributions in prismatic channels are highly recommended.

Acknowledgements Mr. Th. van der Kaaij of Deltares is gratefully acknowledged for performing and analysing the three-dimensional Delft3D simulations on salt intrusion. We also thank Dr. Thijs van Kessel of Deltares for supplying the model results of the three-dimensional simulations on salt intrusion in the Scheldt estuary.

Appendix A: derivation of model equations

Starting from a local approach for the dispersion coefficient in convergent channels ($1<L_a/L_e<10$) D_x is expressed as:

$$D_x = c_1\sqrt{\pi}\left(\frac{v_{\Delta,x}}{\widehat{u}_x}\right)\left(\frac{C^2}{g}\right)^{\alpha_2}\left(\frac{|u_{r,x}|}{\widehat{u}_x}\right)^{0.5}\frac{L_{e,x}}{L_a}\widehat{u}_x h_x \qquad \left(1<\frac{L_a}{L_{e,x}}<10\right) \tag{26}$$

with

$$v_{\Delta,x} = \sqrt{\frac{\Delta\rho_x}{\rho}gh_x} \tag{27}$$

$$u_{r,x} = \frac{Q_r}{A_x} \tag{28}$$

$$\widehat{u}_x = \widehat{u}_0\exp(\delta_u x) \tag{29}$$

$$\Delta\rho_x = c_x S_x \tag{30}$$

$$h_x = h_0\ \exp(\gamma x) \qquad \gamma = \tfrac{1}{L_b}-\tfrac{1}{L_a} \tag{31}$$

$$L_{e,x} = L_{e,0}\exp(\delta_u x) \tag{32}$$

Substitution of Eqs. 27, 28, 29, 30, 31 and 32 in Eq. 26 results in:

$$D_x = \left(e^{\left(\frac{\delta_u}{2}+\frac{3\gamma}{2}+\frac{1}{2L_a}\right)x}\right)\sqrt{\frac{c_x}{c_0}}D_0\sqrt{\frac{S_x}{S_0}} \tag{33}$$

Author's personal copy

with $\sqrt{c_x/c_0} \simeq 1$ in Eq. 33. Φ is defined by:

$$\Phi = \frac{\delta_u}{2} + \frac{3\gamma}{2} + \frac{1}{2L_a} \tag{34}$$

so that D_x can be written as:

$$D_x = e^{\Phi x} D_0 \sqrt{\frac{S_x}{S_0}} \tag{35}$$

It is noted that Φ changes to $\Phi = \delta_u/2 + 5\gamma/3 + 1/(2L_a)$ if $C = h^{1/6}/n$ with n the Manning coefficient ($m^{-1/3}$ s).

Differentiating D_x with respect to x gives:

$$\frac{dD_x}{dx} = D_0 \Phi e^{\Phi x} \sqrt{\frac{S_x}{S_0}} + \frac{1}{2\sqrt{S_x}} \frac{1}{\sqrt{S_0}} \frac{dS_x}{dx} D_0 e^{\Phi x} = \Phi D_x + \frac{D_x}{2S_x} \frac{dS_x}{dx} \tag{36}$$

The one-dimensional tide-averaged transport equation for salt is written as:

$$\frac{1}{S_x} \frac{dS_x}{dx} = -\frac{|Q_r|}{A_x D_x} \tag{37}$$

Equations 36 and 37 result in the following linear differential equation for D_x:

$$\frac{dD_x}{dx} = \Phi D_x - \frac{|Q_r|}{2A_x} = \Phi D_x - \frac{|Q_r|}{2A_0} e^{\frac{x}{L_a}} \tag{38}$$

The solution of Eq. 38 is given by:

$$\frac{D_x}{D_0} = e^{\Phi x} + \frac{|Q_r|}{2A_0 D_0} \frac{L_a}{1 - \Phi L_a} \left(e^{\Phi x} - e^{\frac{x}{L_a}} \right) \tag{39}$$

Combining Eqs. 35 and 39 results in the salinity distribution given by:

$$\sqrt{\frac{S_x}{S_0}} = e^{-\Phi x} \frac{D_x}{D_0} = 1 + \frac{|Q_r|}{2A_0 D_0} \frac{L_a}{1 - \Phi L_a} \left(1 - e^{\left(\frac{1 - \Phi L_a}{L_a}\right) x} \right) \tag{40}$$

If the dimensionless parameter ζ is defined according to:

$$\zeta = \frac{1}{1 - \Phi L_a}, \tag{41}$$

Equation 40 can be written as:

$$\frac{S_x}{S_0} = \left[1 - \frac{1}{2} \frac{|Q_r| \zeta L_a}{A_0 D_0} \left(e^{x/(\zeta L_a)} - 1 \right) \right]^2 \qquad \left(1 < \frac{L_a}{L_{e,x}} < 10 \right) \tag{42}$$

The maximum salt intrusion length follows from the condition that $S=0$ at $x=L_{\max}$:

$$L_{\max} = \zeta L_a \ln \left(1 + 2 \frac{D_0 A_0}{\zeta L_a |Q_r|} \right) \tag{43}$$

Appendix B: calibration of the analytical model

Prismatic case

Calibration was first done using data from experiments in a tidal flume with a length of 101.5 m and a width of 0.67 m. At the downstream end the flume was connected with a basin were the water level variation was imposed according to a sine function. At the upstream end a tidal discharge was used as a boundary condition. The tidal flume represented the Nieuwe Waterweg, a straight channel constructed at the end of the nineteenth century connecting the port of Rotterdam with the North Sea. Horizontal and vertical length scales for the model tests were 640 and 64 resulting in a velocity scale of 8 and a time scale of 80. In a distorted model, the Chézy roughness scales with the square root of the distortion which is the ratio of the horizontal and vertical length scales. Thus roughness was increased by means of additional artificial elements (the Chézy value is inversely related to the roughness). Conditions were varied over a wide range resulting in 35 model tests, see Table 2 for minimum and maximum values after conversion to prototype values.

If Eqs. 12b and 12c are used in combination with Eq. 23 with α_1=1 and α_3=0.5 the constant c_2 and the power α_2 can be computed, because the tidal velocity amplitude $\widehat{u}_0$, the water depth h_0, the river flow velocity u_r, the density difference $\Delta\rho$ and the fresh water density ρ_r are all known from the model tests. The tidal amplification or damping, δ_u, was not presented in the original report of Rigter (1971) but here its value is computed for each model test using the linear equations for tidal propagation in a rectangular channel with a finite length (see e.g. Dronkers 2005 and Van Rijn, Part I). These computations are done for a channel with a length L which is larger than the actual flume length L_{flume} (=101.5 m). At the closed end $x=L$ the tidal discharge is nil and the tidal wave is reflected. In a similar way Rigter computed the tidal discharge at the location of the landward boundary of the tidal flume using some hydrodynamic model. The length L was chosen in such a way that the tidal discharge in the mouth of the flume resembled that of the tidal discharges in the prototype. For most experiments, L amounted 179 m but as part of the systematic investigations the length was varied between 106 and 303 m to assess the effect of the tidal velocity in the estuary mouth on salt intrusion.

Figure 4 compares observed maximum salt intrusion lengths with calibrated values for c_2=2.0 and α_2=0.5. From scaling considerations it follows that c_2 scales with the square root of the distortion (i.e. the ratio of the length and vertical scales). As the distortion for the model experiments in the tidal flume was ten the constant c_2 amounts to six for prototype conditions. Now, c_2 and α_2 are known the

Author's personal copy

Table 2 Conditions for experiments in Delft tidal flume on prototype scale (based on Rigter 1973)

			Base test	Minimum value	Maximum value	No. of tests
Water level amplitude	$\hat{\eta}_0$	(m)	0.8	0.4	2.4	6
Roughness	C	($m^{1/2}/s$)	60	40	90	5
Tidal velocity in mouth	$\hat{u}_0$	(m/s)	0.93	0.51	1.68	7
River discharge	$\lvert Q_r \rvert$	(m^3/s)	946	472	3,789	6
Water depth	h_0	(m)	13.8	10.0	18.0	5
Relative density difference	$\Delta\rho/\rho$	(−)	0.0215	0.0045	0.0355	5

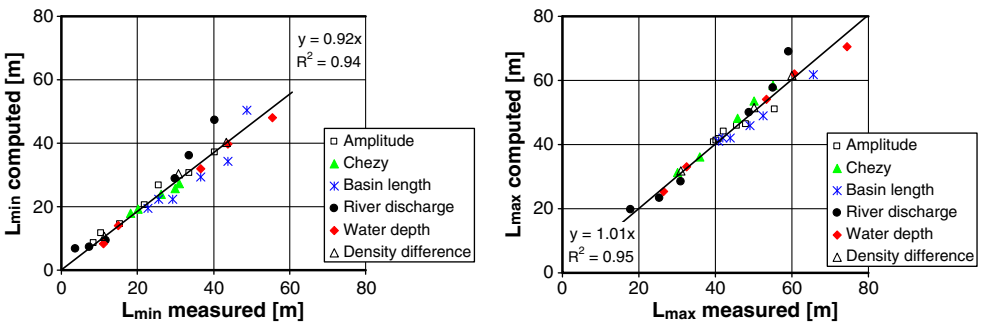

Fig. 13 Measured versus computed salt intrusion lengths for the experiments in the tidal flume. *Left window*, minimum intrusion length according to Eq. 44. *Right window*, maximum intrusion length following from Eqs. 44 and 45

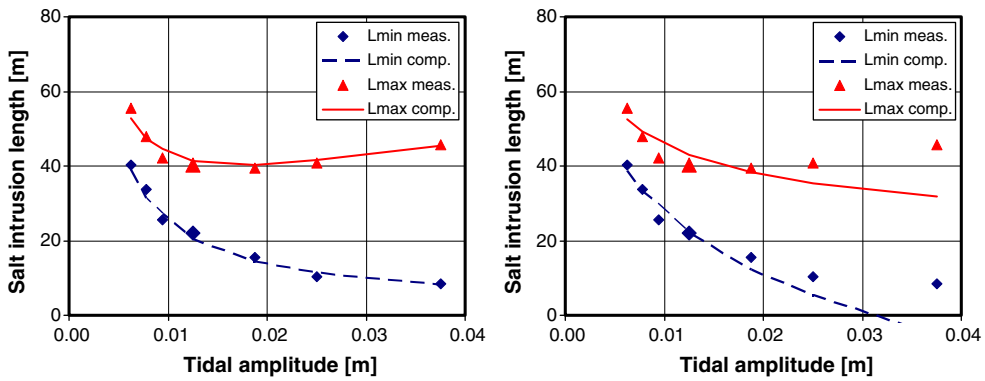

Fig. 14 Maximum and minimum salt intrusion length as a function of the tidal amplitude (on model scale). Comparison between experimental results in tidal flume. *Left window*, $L_{\min}$ and $L_{\max}$ according to Eqs. 44 and 45. *Right window*, $L_{\max}$ according to Eq. 23 and $L_{\min} = L_{\max} - L_{e,0}$

Table 3 Estuaries used during calibration of the model

Estuary	Date	L_{a1} and L_{a2} (km)	L_{b1} and L_{b2} (km)	x_1 (km)	T (s)	h_0 (m)	$\bar{\eta}_0$ (m)	C^a ($m^{0.5}/s$)	$\hat{u}_0{}^a$ (m/s)	$\lvert Q_r \rvert$ (m^3/s)	S_0 (-)	A_0 (10^3 m^2)	N_R (-)	D_0 (m^2/s)	Reference
Lalang	201089	217	96	–	86,400	10.6	1.3	60	0.63	120	27	2.55	1.3	830	Savenije (1992, 2005)
Limpopo	311282	12, 72	12, 72	14	44,400	7.0	0.55	80	0.52	10	36	2.6	0.16	290	Savenije (1992, 2005)
Limpopo	220483	12, 72	12, 72	14	44,400	7.0	0.25	80	0.27	8	33	2.6	0.91	290	Savenije (1992, 2005)
Tha Chin	160481	22, 87	16, 87	22	86,400	5.3	0.8	45	0.43	55	30	3.0	0.91	470	Savenije (1992, 2005)
Tha Chin	270286	22, 87	16, 87	22	44,400	5.3	1.3	45	0.77	40	35	3.0	0.13	325	Savenije (1992, 2005)
Tha Chin	130887	22, 87	16, 87	22	44,400	5.3	1.0	45	0.64	39	32	3.0	0.20	280	Savenije (1992, 2005)
Chao Phya	050662	109	109	–	86,400	7.2	1.1	60	0.62	63	35	4.3	0.37	520	Savenije (1992, 2005)
Chao Phya	290183	109	109	–	86,400	7.2	1.2	60	0.66	90	36	4.3	0.45	810	Savenije (1992, 2005)
Chao Phya	230283	109	109	–	86,400	7.2	0.8	60	0.49	100	31	4.3	1.03	710	Savenije (1992, 2005)
Chao Phya	160187	109	109	–	86,400	7.2	1.25	60	0.68	180	22	4.3	0.51	710	Savenije (1992, 2005)
Incomati	050982	7, 42	7.5, 42	14	44,440	2.9	0.7	60	0.60	2	40	8.1	0.003	20	Savenije (1992, 2005)
Incomati	230693	7, 42	7.5, 42	14	44,440	2.9	0.7	60	0.60	4	37	8.1	0.006	30	Savenije (2005)
Pungue	260980	21, 12	21, 14	38	44,440	3.5	3.15	55	1.32	22	34	28	0.001	240	Savenije (1992, 2005)
Pungue	260582	21, 12	21, 14	38	44,440	3.5	2.5	55	1.11	50	32	28	0.003	150	Savenije (1992, 2005)
Pungue	060882	21, 12	21, 14	38	44,440	3.5	2.6	55	1.14	36	35	28	0.003	140	Savenije (1992, 2005)
Pungue	220982	21, 12	21, 14	38	44,440	3.5	2.6	55	1.15	26	35	28	0.002	160	Savenije (1992, 2005)
Pungue	291082	21, 12	21, 14	38	44,440	3.5	3.0	55	1.28	60	35	28	0.003	230	Savenije (1992, 2005)
Pungue	121093	21, 12	21, 14	38	44,440	3.5	1.9	55	0.90	10	40	28	0.002	80	Savenije (2005)
Corantijn	160865	19, 64	19, 48	18	44,440	6.5	1.1	75	0.84	680	36	69	0.10	410	Savenije (1992, 2005)
Corantijn	141278	19, 64	19, 48	18	44,440	6.5	1.15	75	0.87	130	24	69	0.01	100	Savenije (1992, 2005)
Corantijn	201278	19, 64	19, 48	18	44,440	6.5	0.8	75	0.66	220	20	69	0.04	175	Savenije (1992, 2005)
Delaware	041032	41, 41	42, 42	18	44,440	6.6	0.85	65	0.62	72	35	255	0.007	64	Savenije (1992, 2005)
Scheldt	1075	26, 26	50, 28	50	44,440	12.0	2.0	60	0.73	60	31	168	0.01	290	Savenije (1992, 2005)
Minimum		7	7.5		44,400	2.9	0.25	45	0.27	2	22	2.55	0.001	20	
Maximum		217	109		86,400	12.0	3.15	80	1.32	680	40	255	1.3	830	

[a] Computed according to Van Rijn (part I) using the width convergence length of the landward branch (if applicable)

Author's personal copy

Author's personal copy

dispersion coefficient D_0 can be computed from Eq. 12b as all other quantities in the equation have been measured.

Before the analytical model is applied to convergent estuaries (see hereafter) we will explore an approach that is based on an analysis of the minimum intrusion length. The results of the model experiments with varying tidal amplitude show that with increasing amplitude first the maximum intrusion length decreases from 55 to 39 m and then increases to 46 m, see the data points marked with squares in Fig. 4. The model however predicts a continuous decrease with increasing tidal amplitude. In accordance with expressions given by Schijf and Schönfeld (1953) for an arrested salt wedge and Prandle (1985) and Van Os (1993) for mean and minimum intrusion lengths the following equation is assumed for the minimum salt intrusion length ($L_{\min}$):

$$L_{\min} = c_3 \left(\frac{\nu_\Delta}{\widehat{u}_0}\right)^{\alpha_1} \left(\frac{C^2}{g}\right)^{\alpha_2} \left(\frac{\widehat{u}_0}{|u_{r,0}|}\right)^{\alpha_3} h \tag{44}$$

with α_1, α_2 and α_3 constants that need further assessment. The functional shape according to Eq. 44 is similar to Eq. 23 for the maximum intrusion length in a prismatic

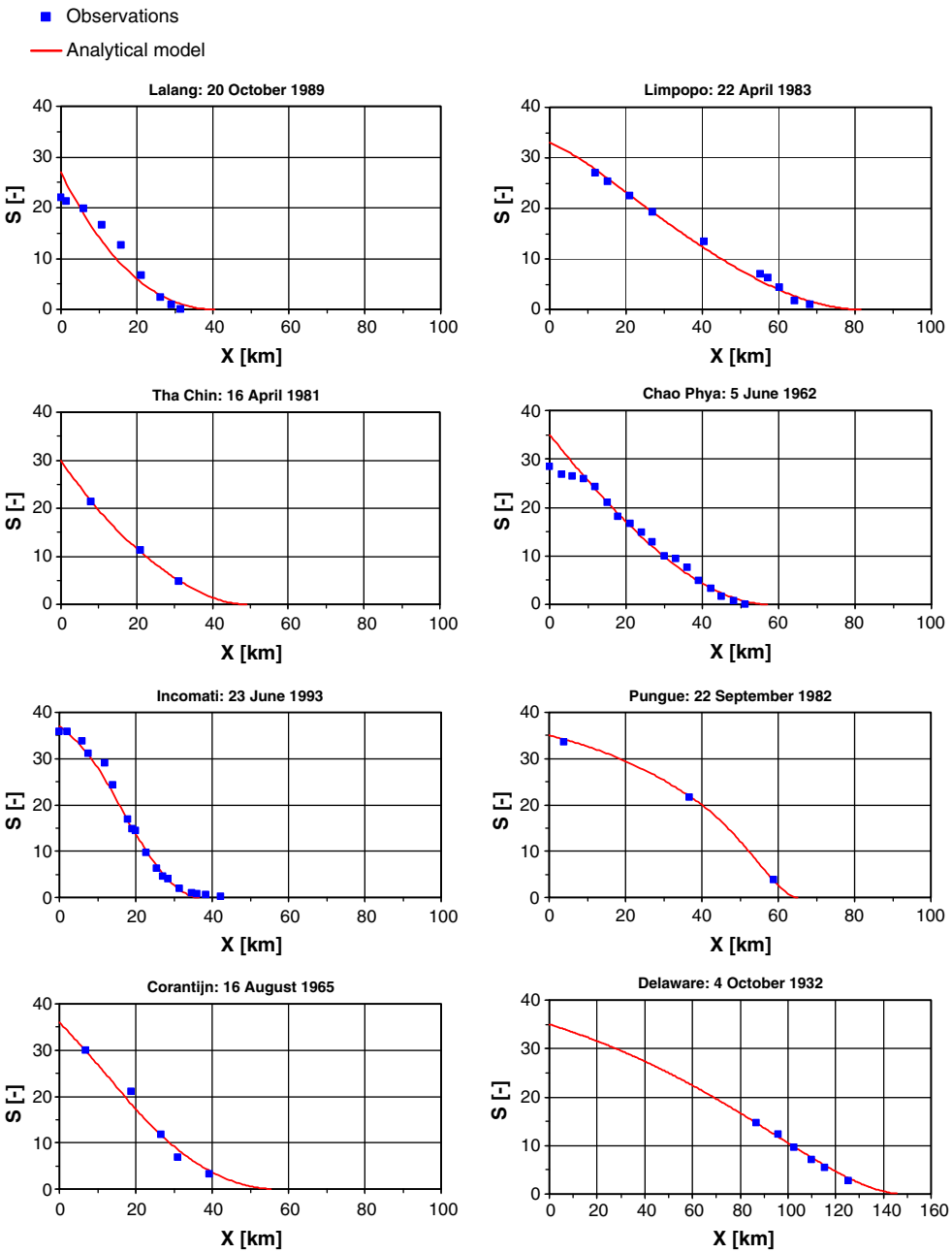

Fig. 15 Salinity distributions for estuaries based on calibration

Author's personal copy

channel if $\delta_u AD_0/|Q_r|<<1$ and using Eq. 12b for D_0. This condition is generally applicable to the tidal flume experiments. The maximum salt intrusion length is subsequently computed with:

$$L_{\max} = L_{\min} + L_{e,0} \tag{45}$$

Multiple regression using data from the tidal flume experiments results in $\alpha_1 = 2.8 \pm 0.13$, $\alpha_2 = 1.0 \pm 0.03$ and $\alpha_3 = 1.3 \pm 0.06$. The standard error of the α values is relatively small (3–5%) resulting in a high regression coefficient r^2=0.98. In Fig. 13, measured and computed values for $L_{\min}$ are compared. The figure also shows measured and computed maximum salt intrusion lengths ($L_{\max}$) with computed values derived from Eq. 45. Minimum and maximum salt intrusion lengths are very well reproduced and it can be concluded that both intrusion lengths are mutually related through the tidal excursion length.

Figure 14 (left window) shows that the effect of an increased tidal amplitude on the maximum intrusion length is correctly reproduced, i.e. if the tidal amplitude becomes larger the maximum intrusion length first decreases due to enhanced tidal mixing and then increases resulting from a larger tidal excursion length. Equation 23 cannot account for this as the computed maximum intrusion length monotonously decreases with increasing tidal amplitude, see Fig. 14, right window). The expression for the minimum intrusion length however performs less well if used for convergent estuaries and it is not further applied here. Additional research is needed to combine the merits of both approaches.

Convergent case

Input data on geometric and hydrodynamic conditions for the estuaries used for calibration are listed in Table 3. These data have been obtained from Savenije (1993a, 2005) and were in some cases slightly modified. This holds for the converging lengths L_a and L_b which were determined from the graphs on width and cross-sectional area along the estuary as presented by Savenije (1992), the Chézy roughness C and the salinity in the estuary mouth S_0 which was not always exactly known. In total, 23 data sets in nine estuaries have been used for calibration and computations have been done with a simple spreadsheet. The minimum and maximum values of the parameters are also given in Table 3. Comparison between observations and model computations is shown in Fig. 15 for some data sets.

Figure 15 shows that the model is very well capable in reproducing the observed salinity distributions with properly chosen values of the dispersion coefficient D_0.

References

Allersma E (1994) Geulen in estuaria. 1-D modellering van evenwijdige geulen. Report H1828, Delft Hydraulics, Delft.

Chatwin PC (1976) Some remarks on the maintenance of the salinity distribution in estuaries. Estuar Coast Mar Sci 4:555–566

Chen Z, Li J, Shen H, Zhanghua W (2001) Yangtze River of China: historical analysis of discharge variability and sediment flux. Geomorphology 41:77–91

Chen X, Zhang E, Xu J (2002) Large and episodic decrease of water discharge from the Yangtze River to the sea during the dry season. Hydrol Sci 47(1):41–48

Dronkers J (2005) Dynamics of Coastal Systems. Advanced Series on Ocean Engineering 25, World Scientific, Singapore, 519 pp.

Elder JW (1959) The dispersion of marked fluid in turbulent shear flow. J Fluid Mech 5:544–560

Fischer HB (1972) Mass transport mechanisms in partially stratified estuaries. J Fluid Mech 53(4):671–687

Fischer HB, List EJ, Koh RCY, Imberger J, Brooks NH (1979) Mixing in inland and coastal waters. Academic, New York

Hunt JN (1964) Tidal oscillations in estuaries. Geophys J R Astron Soc 8:440–455

Ippen A (1966) Salt intrusion in estuaries. In: Ippen AT et al (eds) Estuaries and coastline hydrodynamics. McGraw-Hill, New York

Ippen AT, Harleman DRF (1961) One-dimensional analysis of salinity intrusion in estuaries. Technical bulletin no. 5, Committee on Tidal Hydraulics, Corps of Engineers, U.S. Army.

Jay DA, Geyer WR, Uncles RJ, Vallino J, Largier J, Boynton WR (1997) A review of recent developments in estuarine scalar flux estimation. Estuaries 20(2):262–280

Keulegan GH (1966) The mechanism of an arrested saline wedge. In: Ippen AT et al (eds) Estuaries and coastline hydrodynamics. McGraw-Hill, New York

Kuijper C (1984) Inregeling, ijking en verificatie van de waterbeweging en zoutverdeling in het Getijmodel Rijnmond. Report M2000-3, Delft Hydraulics, Delft

MacCready P (2004) Toward a unified theory of tidally-averaged estuarine saline structure. Estuaries 27(4):561–570

MacVean LJ, Stacey MT (2011) Estuarine dispersion from tidal trapping: a new analytical framework. Estuar Coast 34:45–59. doi:10.1007/s12237-010-9298-x

Nguyen AD, Savenije HHG, van der Wegen M, Roelvink D (2008) New analytical equation for dispersion in estuaries with a distinct ebb-flood channel-system. Estuar, Coas Shelf Sci 79:7–16

Prandle D (1981) Salinity intrusion in esturies. J Phys Oceanogr 11:1311–1324

Prandle D (1985) On salinity regimes and the vertical structure of residual flows in narrow tidal estuaries. Estuar, Coas Shelf Sci 20:615–635

Prandle D (2004) Salinity intrusion in partially mixed estuaries. Estuar Coast Shelf Sci 54:385–397

Prandle D (2009) Estuaries. Dynamics, mixing, sedimentation and morphology. Cambridge University Press, Cambridge

Prandle D, Rahman M (1980) Tidal response in estuaries. J Phys Oceanogr 10:1552–1573

Rigter BP (1971) Reproductie zouttoestand getijrivieren. Dimensie analyse zoutindringing. Systematisch onderzoek. Report M896-XV, Waterloopkundig Laboratorium.

Rigter BP (1973) Minimum length of salt intrusion in estuaries. In: Proceedings of the American Society of Civil Engineers 99, No HY9. Journal of the Hydraulics Division

Author's personal copy

Savenije HHG (1986) A one-dimensional model for salinity intrusion in alluvial estuaries. J Hydrol 85:87–109

Savenije HHG (1989) Salt intrusion model for high-water slack, low-water slack, and mean tide on spread sheet. J Hydrol 107:9–18

Savenije HHG (1993a) Predictive model for salt intrusion in estuaries. J Hydrol 148:203–218

Savenije HHG (1993b) Composition and driving mechanisms of longitudinal tidal average salinity dispersion in estuaries. J Hydrol 144:127–141

Savenije HHG (2005) Salinity and tides in alluvial estuaries. Elsevier, Amsterdam, p 194

Savenije, H HG (1992) Rapid Assessment Technique for Salt Intrusion in Alluvial Estuaries. Ph.D. thesis. IHE report series, no. 27. International Institute for Infrastructure, Hydraulics and Environment, Delft, The Netherlands.

Schijf JB, Schönfeld JC (1953) Theoretical considerations on the motion of salt and fresh water. In: Proceedings Minnesota International Hydraulics Convention. IAHR and Hydraulics Division ASCE, pp. 321–333.

Simpson JH, Brown J, Matthews J, Allen G (1990) Tidal straining, density currents, and stirring in the control of estuarine stratification. Estuaries 13:125–132

Taylor G (1954) The dispersion of matter in turbulent flow through a pipe. Proc Royal Soc A 223:446–468

Toffolon M, Crosato A (2007) Developing macroscale indicators for estuarine morphology: the case of the Scheldt estuary. J Coast Res 23(1):195–212

Uncles RJ, Stephens JA, Smith RE (2002) The dependence of estuarine turbidity on tidal intrusion length, tidal range and residence time. Cont Shelf Res 22:1835–1856

Van der Burgh P (1972) Ontwikkeling van een methode voor het voorspellen van zoutverdelingen in estuaria, kanalen en zeeën. Rijkswaterstaat, Report 01–72.

Van Kessel T, Vanlede J (2010) Impact of harbour basins on mud dynamics Scheldt estuary. In the framework of LTV. Report 1200253, Deltares and Flanders Hydraulics Research.

Van Os, A.G. (1993) Density currents and salt intrusion. Lecture notes IHE, Delft, The Netherlands

Van Rijn LC 1990, 2011. Principles of fluid flow and surface waves in rivers, estuaries, seas and oceans. Aqua Publications, Amsterdam, The Netherlands. Available at: (www.aquapublications.nl).

Van Rijn, L.C., 2011. Analytical and numerical analysis of tides and salinities in estuaries. Part I: Tidal wave propagation in convergent estuaries. Estuar Coast Shelf Sci (in press)

Xue P, Chen C, Ding P, Beardsley RC, Lin H, Ge J, Kong Y (2009) Saltwater intrusion into the Changjiang River: a model-guided mechanism study. J Geophys Res 114:C02006. doi:1029/2008JC004831